CHALMERS
UNIVERSITY OF TECHNOLOGY

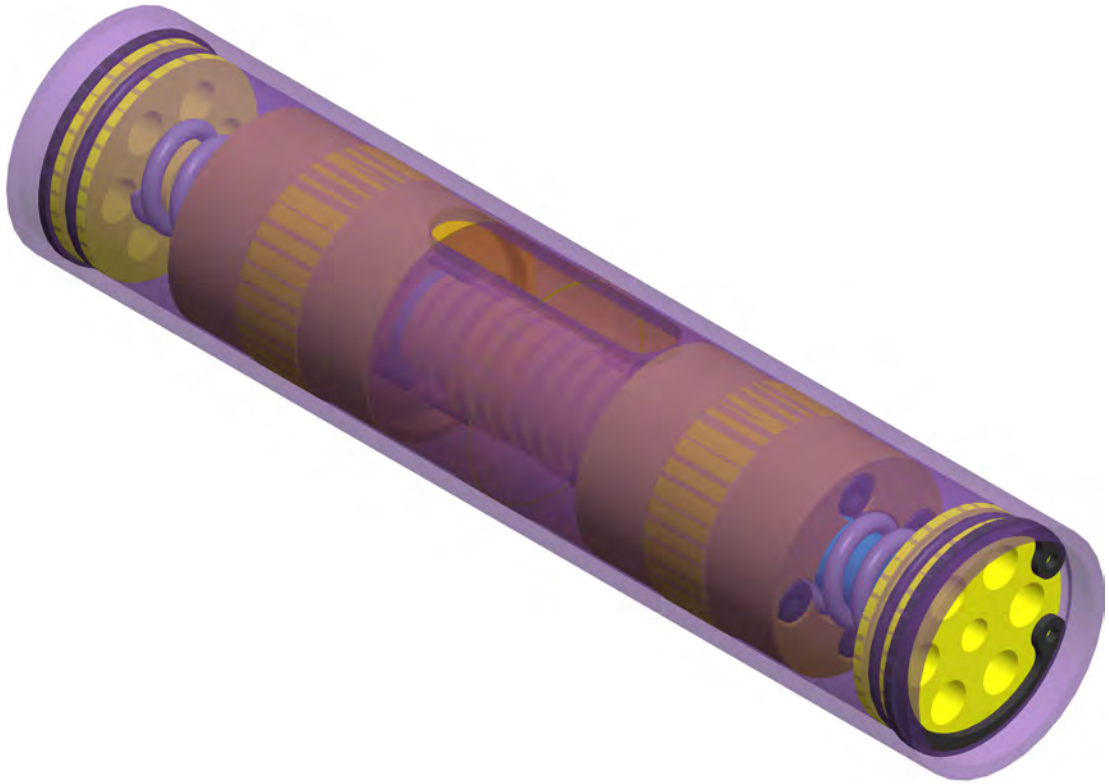

Auto Tuned Vibration Absorber for Reciprocating Saw

Vibration dynamics modelling, simulation and analysis

Master's thesis in Applied Mechanics

Anjan Nagaiah Bhagavan

Department of Mechanics and Maritime Sciences
CHALMERS UNIVERSITY OF TECHNOLOGY
Gothenburg, Sweden 2020

Master's thesis 2020:27

Auto Tuned Vibration Absorber for Reciprocating Saw

Vibration dynamics modelling, simulation and analysis

Anjan Nagaiah Bhagavan

CHALMERS
UNIVERSITY OF TECHNOLOGY

Department of Mechanics and Maritime Sciences
Division of Dynamics
Chalmers University of Technology
Gothenburg, Sweden 2020

Auto Tuned Vibration Absorber for Reciprocating Saw
Vibration dynamics modelling, simulation and analysis
Anjan Nagaiah Bhagavan

Supervisor: Hans Lindell, RISE IVF AB
Examiner: Viktor Berbyuk, Department of Mechanics and Maritime Sciences

Master's Thesis 2020:27
Department of Mechanics and Maritime Sciences
Division of Dynamics
Chalmers University of Technology
SE-412 96 Gothenburg
Telephone +46 31 772 1000

Cover:Prototype model of Auto Tuned Vibration Absorber (ATVA)

Typeset in LaTeX
Gothenburg, Sweden 2020

Auto Tuned Vibration Absorber for Reciprocating Saw
Vibration dynamics modelling, simulation and analysis
Master Thesis in Applied Mechanics
Anjan Nagaiah Bhagavan
Department of Mechanics and Maritime Sciences
Division of Dynamics
Chalmers University of Technology

Abstract

This thesis work investigates an Auto Tuned Vibration Absorber(ATVA) developed by RISE IVF AB for a reciprocating saw (SR 30-A36). ATVA is a tuned vibration absorber whose stiffness exhibits non-linear behaviour. The project aim was to develop an ATVA prototype for reciprocating saw wherein the system parameters of ATVA are tuned for optimal vibration suppression. The entire work was emphasized on measurement of excitation force, optimization of system parameters, prototype development of ATVA.

Prototype development was based on measurements of the excitation force experienced by reciprocating saw while freely running, cutting chipboard and metal-pipe. Actual measurement data was used as input to the simulations and optimization. Further, optimizations were carried out in MATLAB and ADAMS software was used to verify the response obtained.

Non-linear stiffness in ATVA is constructed using two linear springs with a gap between them. Earlier, ATVA with a linear spring and gap was used in a prototype and the system had problems getting activated when connected to reciprocating saw. In this thesis work, the main idea to solve the problem of activation was by using an additional spring in the prototype which can activate ATVA as soon as the system gets excited. Optimizations were performed to identify the two spring stiffness required, the gap between them and the auxiliary mass value for optimal vibration attenuation. Finally the activation of ATVA was verified by simulating the operating conditions.

Keywords: Auto Tuned Vibration Absorber (ATVA), Reciprocating saw, non-linear stiffness, linear spring

PREFACE

This master's thesis is submitted as the final requirement for my master's degree in Applied Mechanics from Chalmers University of Technology. This project was executed during a period of 20 weeks, from January 2020 to June 2020. It was conducted on behalf of and in close cooperation with RISE IVF AB, a Swedish research institute within production and product development. The project was supervised by Lic. Eng. Hans Lindell and Professor Viktor Berbyuk was my examiner at Chalmers.

ACKNOWLEDGEMENTS

The credits of making this project sail towards success goes to my supervisor Hans Lindell and examiner Viktor Berbyuk. I am very thankful to my supervisor for giving me an opportunity to carry out this project at RISE IVF AB. I am greatly benefited from Snævar Leó Grétarsson and I thank him for helping me out in doing various measurements in lab. I appreciate Professor Håkan Johansson for extending his generous support. I also thank Magnus Lövgren for his support in developing ATVA Prototype. I thank all five of you for your constant support through out the project.

Finally, I express my sincere gratitude to my parents, friends and the faculties in the Chalmers University of Technology for providing constant support and continuous encouragement throughout my studies and through the process of researching and writing this thesis. This accomplishment would not have been possible without their support. Thank you.

Anjan Nagaiah Bhagavan, Gothenburg, June 2020

Contents

List of Figures

Nomenclature

Variables

Symbol	Description	Dimensions	Units
c_a	Damping at Auxilliary mass	MT^{-1}	Ns/m
c_m	Main Damping	MT^{-1}	Ns/m
c_p	Human Hand Damping	MT^{-1}	Ns/m
F_0	Preload	MLT^{-2}	kN
$F_{e,RS}$	Excitation Force	MLT^{-2}	N
f_{lb}	Lower Bound Frequency	T^{-1}	1/s
f_{ub}	Upper Bound Frequency	T^{-1}	1/s
f_{nom}	Nominal Frequency	T^{-1}	1/s
f_{ref}	Reference Frequency	T^{-1}	1/s
k_1	Linear Stiffness (Soft Spring)	MT^{-2}	kN/m
k_2	Linear Stiffness (Hard Spring)	MT^{-2}	kN/m
k_a	Non Linear Stiffness	MT^{-2}	kN/m
k_m	Main Stiffness	MT^{-2}	kN/m
k_p	Human Hand Stiffness	MT^{-2}	kN/m
m_a	Auxiliary mass	M	kg
m_m	Mass of Reciprocating Saw	M	kg
t_s	Sweep time	T	s

Abbreviations

ATVA	Auto Tuned Vibration Absorber
FFT	Fast Fourier Transform
FTVA	Fixed Tuned Vibration Absorber
HAVS	Hand Arm Vibration Syndrome
HSLDS	High Static Low Dynamic Stiffness
LTVA	Linear Tuned Vibration Absorber
NLTVA	Non-Linear Tuned Vibration Absorber
RS	Reciprocating saw
WOTVA	Without Tuned Vibration Absorber

1
Introduction

This project was executed in collaboration with Research Institutes of Sweden (RISE IVF AB). Within this project, a computational model of reciprocating saw is developed and a prototype concept of non linear tuned vibration absorber is developed. The project definition, goals and limitations are outlined below.

1.1 Background

Vibrations in power tool is a frequent problem in many industries. Exposure to vibrations generated from the machine tools can cause various vascular and neuromuscular symptoms called as Hand arm Vibration Syndrome(HAVS). The commonly seen vibrations related symptoms in operators are loss of sensitivity, intolerance to cold and numbness in fingers [1]. In this thesis, the focus is on reducing vibrations in Reciprocating saw. Reciprocating saw is widely used in construction industry and workshops. The amount of time spent by the operators using these type of machines on daily basis is roughly 6 to 8 hours. Long vibration exposure time can lead to serious problems in operators and studies has shown that the damage is irreversible [1]. A detailed survey made by L. Aarhus et al shows the neurosensory components of HAVS [2]. Hence, the need for less vibrating power tools in industry is quite high. This project aims at reducing vibration levels on reciprocating saw.

A possible strategy to isolate vibrations in civil structures are to use Tuned Vibration Absorbers(TVA)[3]. Tuned Vibration absorbers are also called as Tuned Mass Dampers. Tuned Mass Damper was patented in 1911 by H.Frahm [4]. TVA are additional degree of freedom added to the main structure. It is a system consisting of small mass and a spring. The system parameters of the absorber such as mass and stiffness are tuned in a such a way that its natural frequency coincides with the external excitation frequency. This causes the absorber mass to move in counter phase to that of the main structure and thus reducing the vibrations. Theoretically, undamped vibration absorbers when tuned can suppress all vibrations at one specific external excitation frequency in the undamped main structure.

The linear TVA become ineffective when the excitation frequency varies by a small proportion. These absorbers are highly sensitive to excitation frequency. They have a very narrow band of vibration supression. A new method to increase the vibration supression region in impact machine (pneumatic breaker) was proposed and a patent was filed by H.Lindell in 2014 [5]

The NLTVA technique was first used in pneumatic breaker and substantial vibration reduction was observed. The system parameters were fine tuned further in the pneumatic breaker to achieve optimum vibration supression [6],[7]. This methodology was tested in a test rig and a prototype of pneumatic breaker proved that the technique was efficient in practical situations. Also investigations were made on other power tools wherein the technique can be adopted to reduce vibrations [8].

1.2 Purpose

The purpose of this master thesis/project is to investigate the vibrations in reciprocating saw during operation and explore how ATVA can reduce vibrations. The following questions has to be addressed,

- How does the reciprocating saw work and what is the source of vibration?
- How does the unbalance in the rotating wheel influence the vibrations in reciprocating saw?
- How to consider the interaction of work-piece and reciprocating saw during cutting action?
- How does ATVA influence on varying external excitation?
- How to induce non-linearity in ATVA, which can aid in vibration suppression? Different methods are investigated to create non-linearity and feasibility of such methods has to be investigated. For example, can a conical spring be used to create non-linearity and thus make ATVA activated at lower amplitudes of vibrations? This involves feasibility studies of the conical spring to ATVA application.

1.3 Limitations

- The cutting forces from cutting action has to be assumed/modelled in a weak sense, since it is hard to measure. Assumptions are made based on findings from the literature.
- The thesis considers only certain range of frequency of excitation and the excitation is harmonic always. This is not the case in real applications.
- The different operating scenarios could affect the final results. For example, the cutting angle, wear in blades, workpiece material.
- Strength analysis or Fatigue analysis of different components in ATVA is not considered in this thesis work.
- The prototype development within the thesis time of 20 weeks could also be a limitation.

2
Theory

In this section, the concepts required for developing the engineering and mathematical models of the reciprocating saw are explained. The theory behind tuned vibration absorber/ tune mass damper is presented.

2.1 Literature Studies

In Literature studies, the idea was to search new technical publications and patents related to passive vibration isolation. The non-linear vibration absorber and its optimization to pneumatic breaker application [7],[6],[5] were studied. Previously performed master thesis on the topic "Investigation of feasibility of Auto Tuning Vibration Absorber" [8] was studied to understand the behaviour of non-linear tuned vibration absorber to reciprocating saws. The above mentioned technical documents was given by Hans Lindell and Viktor Berbyuk to throughly understand the previous work done. With this background, more research was done to find if there are any new novel ways of passive vibration isolation. Primarily, a google search was made on topics related to passive vibration isolation and tuned absorbers. This was followed by google scholar search related to these topics. Later, different technical papers related to linear and non-linear passive vibration absorbers was searched in Science direct via Chalmers Library.

New papers and patents related to NLTVA were searched and no new patent related to NLTVA was found. The search for new papers revealed a technique of using High Static Low Dynamic Stiffness (HSLDS) in vibration isolators [9]. In the PhD thesis of Alessandro Carrella [9] two methods of obtaining non-linear stiffness in vibration isolators are presented. Firstly it is shown that non-linear stiffness can be obtained using oblique arrangement of springs cf.Figure.2.1 and secondly using a pair of magnets and compression springs cf.Figure.2.2. Magnets in attracting and repelling configuration were studied in [9].

The first method is very promising with respect to the non-linear stiffness, but when it comes to manufacturing it is quite hard to obtain such arrangement. Hence the first method presented is not practically possible. The final results shows that the vibration isolators constructed with magnets and compression spring is better when compared to linear isolators in terms of their transmissibility. This system behaves more or less in a linear fashion for small displacements and thus making it suitable for large amplitudes of vibration.

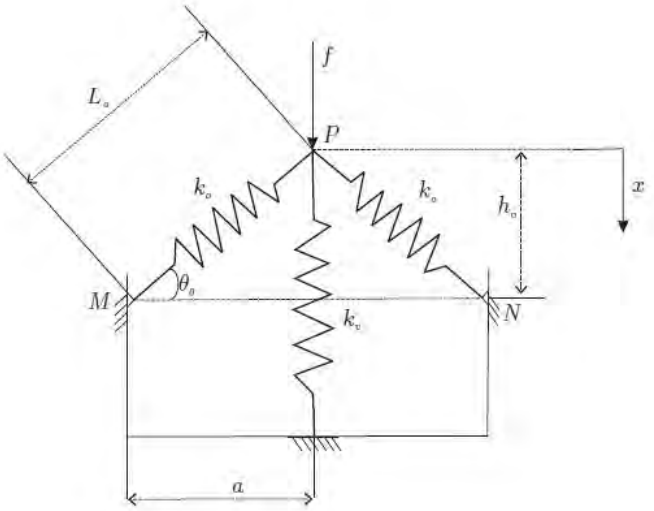

Figure 2.1: *Isolation system with HSLDS system [9]*

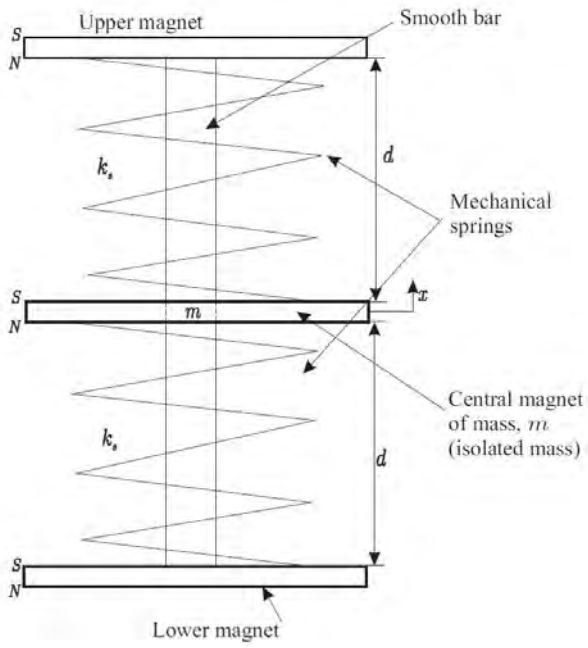

Figure 2.2: *Isolation system with coil spring and magnets [9]*

Literature studies were made related to cutting force generated in sawing process. Cutting forces generated while cutting tropical hard wood was experimentally determined and tabulated in [10]. The studies showed how the cutting force and the wear of the blade is dependent on different varieties of tropical wood. The 3 dimensional forces in cutting at various conditions are presented. This data is useful to understand what magnitude of force one can expect while cutting. The idea is to use these forces for trial simulations to check the model response.

Conical Spring

Conical Springs exhibits non-linear response during compression and this behaviour was studied to identify if conical springs can be used in ATVA. The analytical expressions relating the displacement of the spring and the restoring force is given by E.Rodriguez et al.in [11]. According to the analytical expressions the stiffness has a linear and non-linear region. The force displacement plot exhibits linear region for a smaller displacement and later enters a non-linear region when the displacement exceeds the solid length of the spring. The linear to non-linear transition behaviour shown by conical springs are a good choice for ATVA. But, the disadvantage of using conical spring is that for a given stiffness the size of the conical spring is at least 2 to 2.5 times bigger than normal compression springs [12]. Hence further studies was not carried out with respect to conical springs.

2.2 Tune Mass Damper

Tune mass damping is a passive technique to control vibrations. Tuned Vibration absorbers form an additional degree of freedom (auxiliary system) to the main vibrating system. Here, the term tuned meaning that the vibrating system under consideration is excited by external force at exactly same frequency as that of the natural frequency of the auxiliary system. This method was first introduced by H.Frahm [4] in 1911 and the first first linear tuned vibration absorber theory [13] was written by J.P. Den Hartog in 1956.

A single dof system attached to a auxiliary system is shown in Figure.2.3b with generalized co-ordinates q_1, q_2. The main system is excited by a force which varies harmonically with time, $F(t) = F_a sin(\omega t)$.

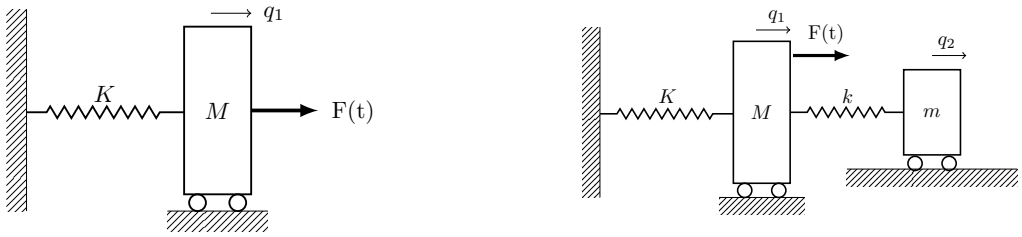

(a) *Undamped single DOF system*

(b) *Undamped single DOF with auxiliary mass*

Figure 2.3: *Undamped vibrating system with generalized co-ordinates q_1,q_2*

In an undamped system, the linear tuned vibration absorber can be tuned to suppress all the motion of the main system by adjusting the eigenfrequency of the tuned absorber to match exactly with the external excitation frequency. The equations of motion for a two degree of freedom system is given in Equation.2.1

$$\begin{aligned} M\ddot{q_1} + (K+k)q_1 - kq_2 &= F_a sin(\omega t) \\ m\ddot{q_2} - kq_1 + kq_2 &= 0 \end{aligned} \tag{2.1}$$

where F_a is the force amplitude and the solution to the Equation.2.1 can be written as,

$$\begin{aligned} q_1(t) = \hat{q_1} sin(\omega t), q_2(t) = \hat{q_2} sin(\omega t) \\ \text{where } \hat{q_1} \text{ and } \hat{q_2} \text{ are vibration amplitudes} \end{aligned} \tag{2.2}$$

The amplitude of vibration can be analytically derived by substituting Equation.2.2 in Equation.2.1 which results in the following [14],

$$\hat{q_2} = \frac{\frac{F_a}{k_1}}{\left(1 - \frac{\omega^2}{\omega_2^2}\right)\left(1 + \frac{k_1}{k_2} - \frac{\omega^2}{\omega_1^2}\right) - \frac{k_2}{k_1}} \tag{2.3}$$

$$\hat{q_1} = \hat{q_2}\left(1 - \frac{\omega^2}{\omega_2^2}\right)$$

From the amplitudes of vibration expression, one can notice in Equation 2.3, $\hat{q_1} = 0$ if $\omega = \omega_2$. This means a total vibration suppression is possible in case of undamped systems.

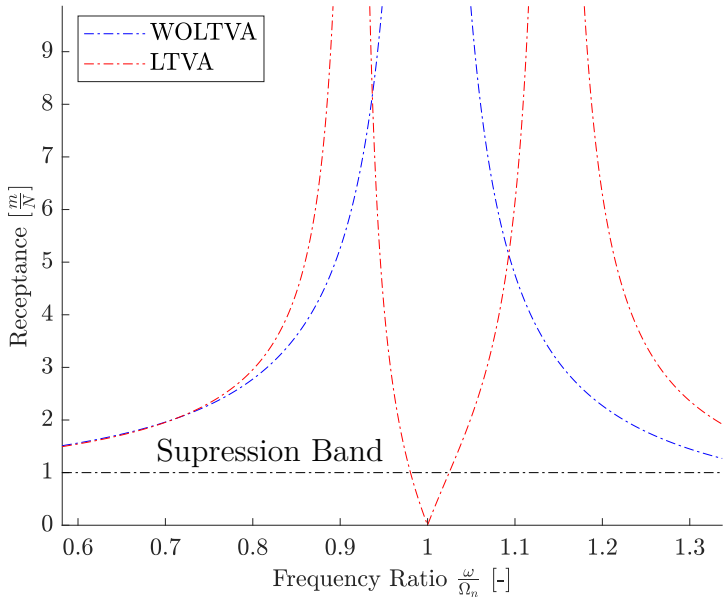

Figure 2.4: *Receptance Plot for undamped system*

The frequency response of main mass for an undamped 1 DOF system and undamped 1 DOF system with auxiliary mass attached is shown in Figure.2.4. In the plot, the frequency ratio is defined as the ratio of external excitation frequency(ω) to natural

frequency of auxiliary system(Ω_N). It can be noticed that, during resonance in 1 DOF system the receptance theoretically goes to infinity, whereas in the presence of auxilliary mass the receptance of main mass is reduced to zero. Note that the suppression band is marked as black dotted line. The effective frequency range of LTVA can be defined for all receptance values below 1. It can be observed that the linear system has a very narrow frequency range. Any change in frequency ratio of $\pm$ 2% makes the LTVA inefficient.

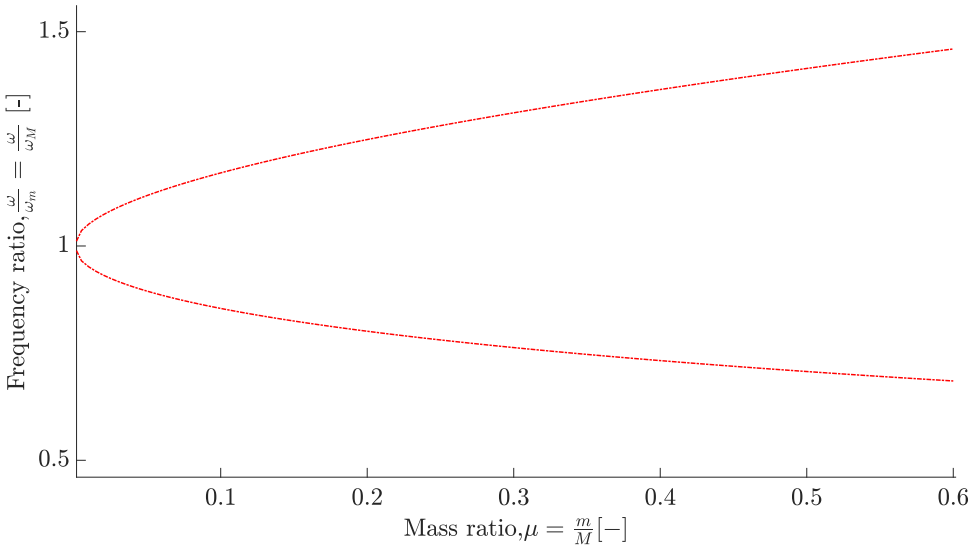

Figure 2.5: *Spread of Eigenfrequencies for different mass ratio when* $\frac{k}{m} = \frac{K}{M}$

The ratio of auxiliary mass to main mass decides the eigenfrequency of the system and thus it is very important to know the behaviour. In Figure.2.5 it can be observed that the two eigenfrequencies of the system are symmetrically spread for different mass ratio when the condition $\frac{k}{m} = \frac{K}{M}$ is met. Note that mass ratio equal to zero means it is one degree of freedom system.

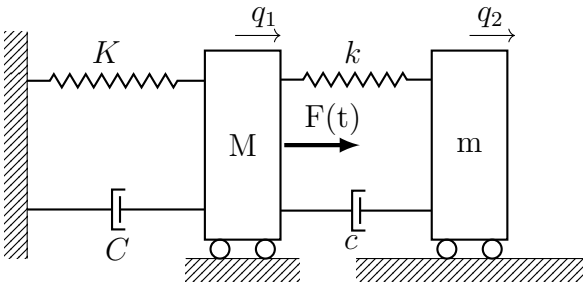

Figure 2.6: *Damped Two Degree of freedom system with generalized co-ordinates* q_1,q_2

The equations of motion for the damped two degree of freedom system shown in Figure. 2.6 is given by

$$\begin{aligned} M\ddot{q_1} + (K+k)q_1 - kq_2 + (C+c)\dot{q_2} - c\dot{q_2} = F_a sin(\omega t) \\ m\ddot{q_2} - kq_1 + kq_2 - c\dot{q_1} + c\dot{q_2} = 0 \end{aligned} \tag{2.4}$$

The frequency response function for a damped absorber was closely investigated in [15] by J. Ormondroyd and J. P. Den Hartog in 1928. They found that the receptance function of the main mass had two invariant points independent of absorber dampening. They proposed to modify the stiffness properties of the absorber such that it forms two fixed points of equal heights in receptance curve. Later, they insisted to select dampening value of the absorber such that it forms tangent to one of the fixed points. This method was called as equal-peak method. This method ensures that the vibration in the main mass is kept low at the resonance frequency. An approximate analytical solution for the absorber stifness and dampening was derived by J. P. Den Hartog [13] and J.E. Brock in [16]. The exact close form solution was later proposed by T. Asami,O. Nishihara, in 2003 [17].

The important point to note is that by adding additional degree of freedom to the main mass, we also introduce a new resonance frequency little higher than the tuned frequency. A linear tuned vibration absorber can supress vibrations at only tuned frequency. The supression band in linear systems is very narrow. So sufficient care has to be taken while designing the linear tuned vibration absorbers with the knowledge of excitation frequency. In many industrial applications, wide range of excitation frequencies limits the usage of linear tuned vibration absorbers. Hence, a non-linear tuned vibration absorber is preferred in this case to accomodate a wider range of external excitation frequencies. The non-linear tuned vibration absorbers created using soft belleville springs demonstrated that the suppression bandwidth can be doubled [18].

2.3 Frequency Response

The frequency domain solutions is very effective in analysing vibration problems concerned with linear systems. The frequency response analysis of linear vibrating systems are based on Fourier assumptions that the time domain solution can be split into spatial and temporal part. Another, important assumption is that the system excitation is stationary harmonic. The stationarity means that the transient vibrations have died out in the considered time frame. The time domain solution to a vibrating mechanical system requires analyzing differential equations whereas the frequency analysis depends on algebra and complex numbers. Also, the computation of resonance frequency and anti-resonance frequency is easier in frequency domain. Further, the duality between time domain and frequency domain is easily established via inverse Fourier transform which gives an easier option to choose when one of the approach is hard.
The frequency response analysis is performed on state space representation of the vibrating mechanical system. The state space approach simplifies the computation by adopting states of the degrees of freedom. Here, the state represent displacement and velocity of each degree of freedom in the vibrating mechanical system. The

frequency response for vibrating mechanical system with n generalized co-ordinates, stimulus $\mathbf{u}$(t) and output $\mathbf{Y}$(t) in state space is given below [14],

$$\begin{aligned} \dot{\mathbf{X}} &= \mathbf{A}\mathbf{X} + \mathbf{B}u \\ \mathbf{X} &= [q_1 \dots q_n, \dot{q_1} \dots \dot{q_n}]^T \\ \mathbf{Y} &= \mathbf{C}\mathbf{X} + \mathbf{D}u \end{aligned} \tag{2.5}$$

where $\mathbf{A}$, $\mathbf{B}$ are system matrices. The transfer function $\mathbf{G}(s)$ for Equation.2.5 is computed by taking Laplace transform of the state space equation and is written as,

$$\mathbf{G}(s) = \frac{\mathbf{Y}(s)}{\mathbf{u}(s)} = \mathbf{C}(s\mathbf{I} - A)^{-1}\mathbf{B} + \mathbf{D} \tag{2.6}$$

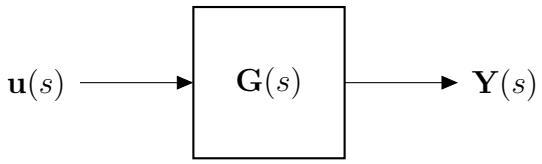

Figure 2.7: *System Transfer Function*

The frequency response of all linear systems can be computed using Equation. 2.6. Transfer function maps input space to an output space and can be realized as a gain function cf. Figure.2.7. The transfer function has different names when different outputs of the state space model is used. For instance, the transfer function is called *receptance* when the output $\mathbf{Y}$ contains displacements. The unit of *receptance* is m/N. If the outputs are velocity and acceleration, then the transfer functions are called as *mobility* and *accelerance* respectively. Unit of mobility is m/Ns and accelerance is m/Ns^2.
In case of Non-linear systems, the system's matrix A and B depend on the states of the system. Hence, the transfer function cannot be computed as given in Equation.2.6. The complex behaviour of non-linear systems are characterized by its super harmonics, sub harmonics, inter-modulation and bifurcation. Mathematical treatment required to analyze frequency response of non-linear systems such as Volterra series expansion can be performed as given in [19]. In this thesis work, the transfer functions are numerically evaluated by calculating the response of non-linear system at each frequency step.

FFT

Fast Fourier transform (FFT) is used to analyse the time domain vibration data obtained from vibration measurements. The Fourier transform of a finite data set, that is Discrete Fourier Transform (DFT) is computed using FFT algorithm. FFT algorithm produces good results when the finite data set starts and ends at same

value. In physical measurements, it is often very difficult to achieve same start and end points. This creates discontinuity in the periodic data set. FFT of data set which are discontinous causes spectral leakage. The actual intensity of peaks are spread out between different frequency bins. To avoid spectral leakage, windowing functions are used. Different windowing functions can be used based on what information has to be analysed from FFT. A brief description of different windowing functions are given in [20] and the same is followed in FFT analysis of measured data. Mainly two window functions such has *flattop* window and *hans* window are used in this thesis work. The window functions are also available as a standard function in Matlab and are called with the same names *(flattop,hans)*. Flat top window enables in estimating true peak intensity values whereas hans window helps in positioning the peaks at respective frequency bins. Also it is suggested to use *hans* window in general for analysis since it eliminates all the discontinuity,[20].

3

The Model

In this section the engineering model and the mathematical modelling of reciprocating saw are described. The methodology followed in developing ADAMS model is presented. The engineering assumptions made in the model is explained. Finally, the mathematical model built in MATLAB is verified against ADAMS model.

3.1 Reciprocating saw

The reciprocating saw works on the principle of slider crank mechanism. An electric motor driven by battery drives a worm gear in the saw which in turn imparts rotational movement to the worm wheel. Worm gears are used to change the rotation axis by 90° since the rotational axis of the electric motor is inline with slider. The bigger worm wheel has a pin which is eccentrically connected to a connecting rod. This connecting rod drives the slider back and forth. A hack saw blade is attached to the slider with a quick release mechanism. The back and forth motion of the slider imitate the cutting action. The cutting action induces vibrations in the tool. To counter balance the cutting forces along the movement of blades, an eccentric mass is added in the rotor. The added mass cause additional vibrations perpendicular to blade motion. The cutting forces generated in the saw are crucial with respect to vibrations and wear of tool. A study was made by Stephen.P Loehnertz and Iris Vazquez to estimate cutting forces generated while cutting different varieties of tropical hardwood [10]. A series of experiments were conducted to identify different components of cutting force. The forces were measured along three directions:parallel, lateral and normal to cut. The results from the measurements indicated that the peak cutting force was 5 times the average cutting force parallel to the cut. A schematic representation of the slider crank mechanism is shown in Appendix A, Figure.A.1 and its kinematic analysis is also presented.

3.2 Engineering model of Reciprocating Saw

The entire reciprocating saw is modelled as one single mass considering as a rigid body, Figure.3.1. This single mass is called as main mass(m_m) from here onwards. The auxilliary system consists of non-linear spring stiffness. Two compression springs are used to obtain the non-linear behaviour by introducing a predefined gap(α) between main mass and auxilliary mass. The main stiffness k_m is modelled as linear spring between the cutting blade and work-piece. In a similar way the interaction of machine with operator is also modelled as linear spring k_p. The damping

between the main mass and work-piece is c_m and damping at the operator interface is c_p. The operator stiffness and damping is adopted from the previous thesis work [7]. The arrangement of linear springs between main mass and auxilliary mass to obtain non-linearity is schematically shown in Figure.3.2,[8]. Note that the walls in the figure represent the main-mass (m_m). In reality, the non-linear spring force can be obtained by placing two compression springs concentrically with a gap α between them. Refer Appendix.C for the actual arrangement of springs (k_1,k_2).

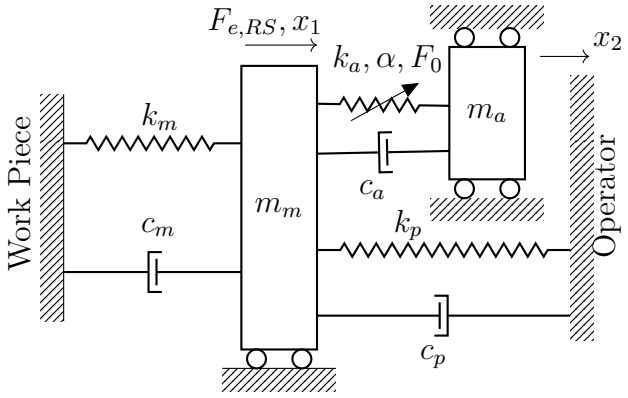

Figure 3.1: *Schematic Representation of Engineering model of Reciprocating saw with ATVA*

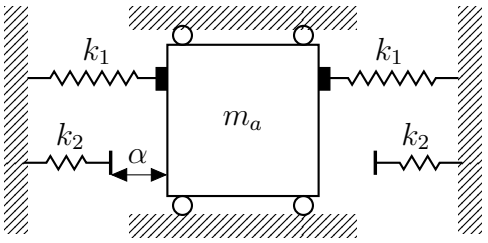

Figure 3.2: *Schematic Representation of Non-linear Auxilliary Mass system [8]*

Non-Linear Stiffness

The non-linear stiffness profile is obtained by combining stiffness of two linear springs with a gap between the first and the second spring. The non-linearity is also present when one of the spring is pre-loaded. In this thesis work, the non-linearity due to pre-loading of spring is not considered. The reason for not considering pre-loading is due to the fact that the pre-load force(F_0) does not influence much in auto-tuning and this was very well seen from the previous work at RISE [7].
Note that the one end connection between the spring stiffness k_1 and auxilliary mass is not fixed (represented as ■ in Figure.3.2). This can be observed in the equations of motion given in Equation.3.3 wherein the spring force generated by spring stiffness k_1 is accounted only once eventhough two springs of stiffness k_1 is shown in the Figure.3.2. An example of the non-linear spring force variation with a gap α is presented for arbitrary k_1, k_2 in Figure.3.3.

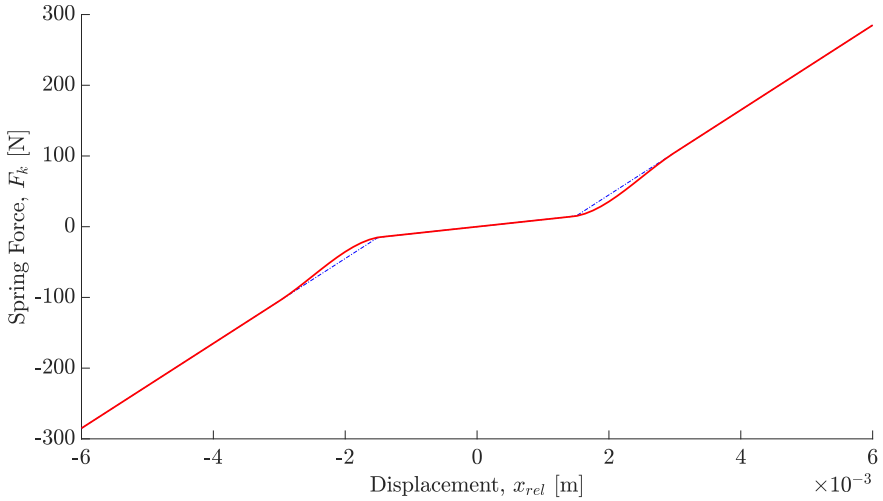

Figure 3.3: *Non-Linear Spring Force Vs Displacement Plot with force smoothening* $[k_1 = 10\,\mathrm{kN/m},\ k_2 = 50\,\mathrm{kN/m},\ \alpha = 1.5\,\mathrm{mm}]$

It has to be noted that the slope of the curve in Figure.3.3 jumps when $x_{rel} = \pm\alpha$. This creates numerical problems while solving differential equations and hence a smooth transition of slope is established via Piecewise Cubic Hermite Interpolating Polynomial(PCHIP). The coefficients of interpolating polynomial is obtained in Matlab by using *pchip* function. This methodology of force curve smoothening was adopted from the previous thesis work [8].

3.3 Mathematical model of Reciprocating Saw

The equations of motion for the engineering model shown in the above section are derived using Lagrange formalism. Viscous force acting in different interface is modelled as viscous damping. This assumption is fair enough since there is a relative sliding friction acting between main mass(m_m) and auxiliary mass(m_a). The equations of motion are later used to compute the response of the system and then to optimize the system parameters for better performance of the absorber.

LTVA

In LTVA, the main mass (Reciprocating Saw) is connected with the Auxiliary system via a constant spring stiffness and damping property. Since all the components in the system behave linearly, the auxiliary mass system is defined as Linear Tuned Vibration Absorber. The equations of motion for LTVA is defined in Equation 3.1.

$$\begin{bmatrix} m_m & 0 \\ 0 & m_a \end{bmatrix} \ddot{\boldsymbol{x}} + \begin{bmatrix} c_m + c_a + c_p & -c_a \\ -c_a & c_a \end{bmatrix} \dot{\boldsymbol{x}} + \begin{bmatrix} k_m + k_a + k_p & -k_a \\ -k_a & k_a \end{bmatrix} \boldsymbol{x} = \begin{bmatrix} F_{e,RS} \\ 0 \end{bmatrix} \tag{3.1}$$

where $F_{e,RS}$ is the excitation force from the reciprocating saw.

ATVA

In ATVA, the main mass (Reciprocating Saw) is connected to the Auxiliary system via non-linear spring stiffness. The non-linear spring stiffness is created by introducing gap. The equations of motion for ATVA is given in Equation 3.2 and the corresponding non-linear spring force is defined in Equation 3.3.

$$\begin{bmatrix} m_m & 0 \\ 0 & m_a \end{bmatrix} \ddot{\boldsymbol{x}} + \begin{bmatrix} c_m + c_a + c_p & -c_a \\ -c_a & c_a \end{bmatrix} \dot{\boldsymbol{x}} + \begin{bmatrix} k_m + k_p & 0 \\ 0 & 0 \end{bmatrix} \boldsymbol{x} = \begin{bmatrix} F_{e,RS} + F_{k,RS} \\ -F_{k,RS} \end{bmatrix} \tag{3.2}$$

where

$$F_k(\boldsymbol{x})_{RS} = F_{k,RS} = \begin{cases} F_0 + k_1 x_{rel} + k_a \left(x_{rel} - \alpha\right) & , x_{rel} > \alpha \\ -F_0 - k_1 x_{rel} - k_a \left(-x_{rel} - \alpha\right) & , x_{rel} < -\alpha \\ k_1 x_{rel} & , -\alpha \leq x_{rel} \leq \alpha \end{cases} \tag{3.3}$$

and

$$k_a = k_1 + k_2 \tag{3.4}$$

In Equation 3.3 the term F_0 is the spring preload and x_{rel} is relative displacement of auxiliary mass with respect to main mass. *Note: In this thesis work the spring pre-load is set to zero since the non-linearity is given by the gap (α) and spring stiffness (k_1,k_2).*

Solution

The Mathematical model for the engineering model defined above is solved numerically in Matlab using the ODE solver *ode45*. In the previous master thesis written by M.Josefsson and S.L.Grétarsson,[7] different ode solvers were used to obtain solutions to non-linear system which was compared to analytical solution and it was found that *ode45x* was fair enough in solving the non-linear differential equation system. With a tightened error tolerance, *ode45* solver in matlab was capable of solving non-linear differential equations of similar kind(Equation.3.2). Also it was suggested to solve the differential equations by checking the limit cycle condition in the phase-space plot with a relative tolerance of 5×10^{-3}. The same strategy was used to solve the differential equations presented in Equation.3.2 to reduce the computation time. The efficiency of the ode solver in matlab depends on how stiff the non-linear differential equations are and how the relative and absolute tolerances has to be set to avoid the integration process to fail. The relative and absolute tolerance used in *ode45* are adopted from previous work,[7] which accounts to 1×10^{-8}. The input excitation force to the engineering model is computed by measuring acceleration on reciprocating saw while freely running, cutting chipboard and metal pipe. Thus making the input to the model more realistic.

ADAMS Model

Multi body simulation software, ADAMS is used in simulating the motion of the engineering model. The ADAMS model is built using rigid bodies representing re-

ciprocating mass(m_m) and auxiliary mass(m_a). The stiffness between main mass (m_m) and the work-piece is modelled as a linear spring using Translational spring-damper option in ADAMS. In a similar way, the stiffness & damping between main mass and operator is also defined(k_p,c_p). The stiffness (k_m, k_p) and damping values (c_m, c_p) are defined as design variable in ADAMS environment. Non-linear stiffness between main mass (m_m) and auxiliary mass (m_a) is defined by spline function. The contribution to spring force from concentric springs (k_1, k_2) is obtained as a vector of forces for small increments of displacement in matlab using *pchip* function. Later these values are given as input to the Translational spring damper element, wherein the stiffness is defined as function of deformation (*Spline:F=f(defo)*) and damping value is entered as constant value using design variable c_a.

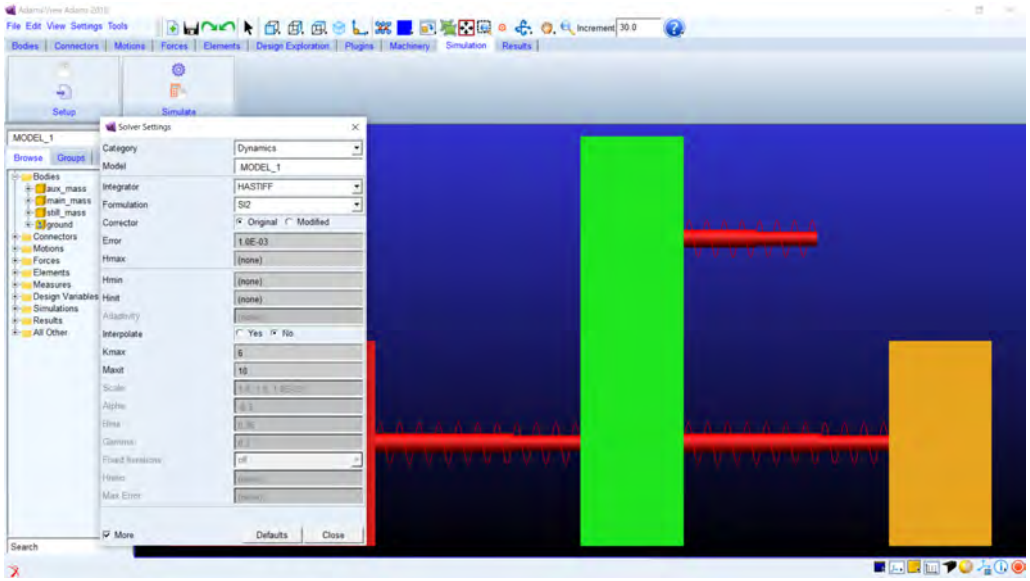

Figure 3.4: *Engineering model in ADAMS software*

In ADAMS, the mathematical model is assembled in the following form,

$$M\ddot{\mathbf{q}} - A^T\mathbf{F}_A(\mathbf{q}, \dot{\mathbf{q}}) + \mathbf{\Phi}_\mathbf{q}^T\lambda = \overline{0}$$

$$\mathbf{\Phi}(\mathbf{q}, t) = \overline{0}$$

where M is the mass matrix, $\mathbf{q}$ is the vector of co-ordinates q_i, A^T is the transformation matrix for projecting forces into different co-ordinates q_i, $\mathbf{F_A}$ is the vector of action forces, $\mathbf{\Phi}$ is the vector of constraint equations, $\mathbf{\Phi}_\mathbf{q}^T$ is the gradient of constraints and λ is vector of Lagrange multipliers.

Output from ADAMS simulation is very much dependent on type of the integrator used. ADAMS has 5 types of time integrators with 3 types of DAE (Differential algebraic system of equations) formulations and the default integrator is GSTIFF (Gear stiff) with I3 formulation. The default integrator is computationally effective but when it comes to solving non-linear problems, GSTIFF integrator becomes

unstable. The proper choice for selecting integrator and its parameters such as integration method, solver formulation, in ADAMS is explained with respect to solution convergence and computational time in [21].

Other available integrators are WSTIFF (Wielenga stiff), HASTIFF (Hiller Anantharaman stiff), HHT (Hilber-Hughes-Taylo), Newmark. All three stiff integrators are robust, multi-step, implicit integrators with variable-order and step size. The difference in the above three integrators lies in its predictor. The common thing among these three stiff integrators are its corrector and they use Backward differentiation formula (BDF). The highest possible order used in BDF is limited to 6. The stiff integrators are also called as stiffly stable integrators, because of the fact that these methods are capable of solving stiff differential equations. In [21] it was suggested that HASTIFF integration method yields faster and accurate results with SI1/SI2 formulation while solving non-linear dynamic system. Hence, in this thesis work, the integration method followed in ADAMS is HASTIFF with SI2 (Stabilized index 2) formulation. All other parameters such as error, maximum iterations, maximum order in the solver is kept to default values, cf.Figure.3.4.

3.4 Model Verification

Parameter	Value	Unit
m_m	4	kg
m_a	0.5	kg
α	1.2	mm
k_m	0.6	kN/m
k_p	0.5	kN/m
k_1	25	kN/m
k_2	40	kN/m
k_{ltva}	39.971	kN/m
c_m	100	Ns/m
c_p	60	Ns/m
c_a	1	Ns/m
F	250	N
f	45	Hz

Table 3.1: Arbitrary Parameters used for model Verification

The computation strategy followed has to be verified with a known result to trust the model response obtained from the Matlab code. In the previous thesis work carried out at RISE, [7], the mathematical model was verified with analytical solution in case of tuned vibration absorber to pneumatic breaker. In this thesis work, the engineering model is built in ADAMS software to visualize the motion. The model response for a known arbitrary parameter set is computed in Matlab and verifed against response in ADAMS. The parameter set used for verifying the model can be seen in Table.3.1. In Table.3.1, k_{ltva} is the stiffness of the auxiliary system which is tuned at 45 Hz and F represents input force amplitude to the E-model. The model response was compared for both linear and non-linear tuned absorbers.

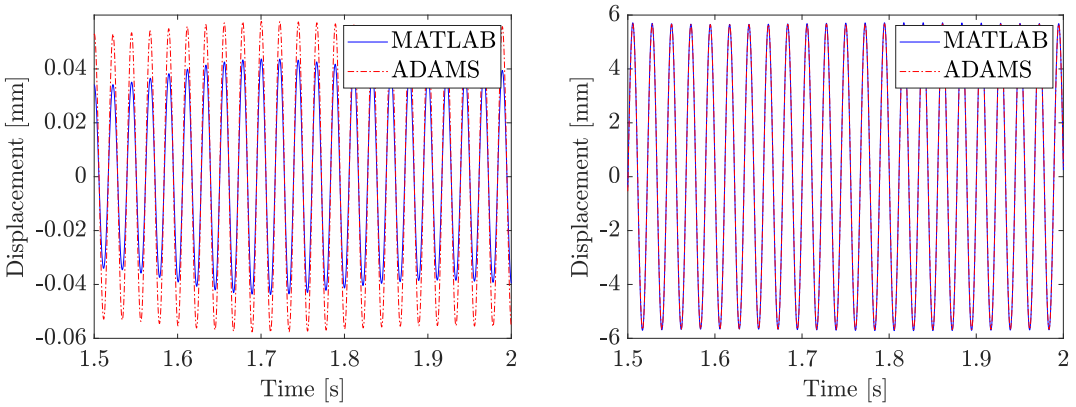

(a) *Main Mass Displacement* **(b)** *Auxiliary mass displacement*

Figure 3.5: *Model verification for Linear Tuned Vibration Absorber*

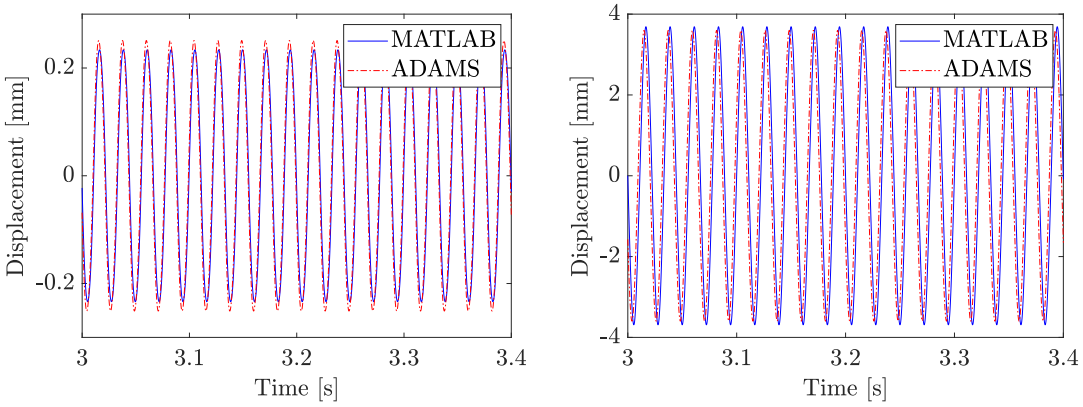

(a) *Main Mass Displacement* **(b)** *Auxiliary mass displacement*

Figure 3.6: *Model verification for Non-linear system at* 45 Hz

With the parameters listed in Table.3.1 the response of the engineering model is compared with ADAMS model for both linear and non-linear system at an excitation frequency $f = 45$ Hz. In case of linear tuned vibration, the stiffness of auxiliary mass is tuned to 45 Hz and the auxiliary mass is set to 0.5 kg to check the model response.

It was observed that the vibration amplitude of main mass differs by 0.014 mm and of auxiliary mass differs by 0.013 mm,cf.Figure.3.5. This shows that both models agree for the arbitrary set of parameters (refer Table.3.1) in linear case. Note that the default integrator GSTIFF with I3 formulation was used in ADAMS whereas *ode45* solver uses adaptive time step with lower error tolerance of 10^{-8} . It can be observed that the response in main mass do not completely match with Matlab results due to the fact that the integrator in ADAMS was set to default error tolerance of 10^{-4}. For the non-linear system, the model built in MATLAB and ADAMS agree very well, cf.Figure.3.6. It was observed that the vibration amplitude of main mass differs by 0.017 mm and that of auxiliary mass by 0.09 mm. In summary, the ADAMS model and the MATLAB model behave similarly for both linear and non-linear stiffness case.

4

Measurements

In this section, the methodology followed in measuring the excitation force acting on reciprocating saw is presented. The measurement results are validated against the engineering model and the parameter sensitivity analysis is shown.

4.1 Excitation Force Measurement

The excitation force acting on the reciprocating saw was measured using two accelerometers. Measurement was taken in three different scenarios.The bottom line was to give in realistic input to the engineering model based on following scenarios,

- Free run
- Chipboard cut
- Metalpipe cut

Firstly, the accelerations in the reciprocating saw during free run was measured. The free run refers to running the machine in air. Measurements in free run were taken when the reciprocating saw was hand held at a horizontal position. Two speed levels were tested at its respective full speed. Secondly, the accelerations in the reciprocating saw was measured while cutting chipboard of standard thickness (38 mm). In this case, the chipboard was mounted on a bench vice in vertical position. Cutting was done along the edge when the saw was held horizontal to ground. The foot rest of the saw was always in contact with the chipboard. Finally, with the same configuration of sensors a metal pipe of outer diameter 50 mm, 2 mm thick was cut. While cutting the metal pipe, the foot rest of the machine was not always in contact with the cutting surface because of the curvature. To compute vibration amplitude, the vibrating motion of the saw was filmed using a high speed camera during free run and the data was analysed in a Tracker software. A detailed description of test setup, video tracking and instruments used is presented in Appendix.B

4.2 Measurement Results

The vibrations on the reciprocating saw were measured as defined above. The measurement results from three cases such as Free Run, Chipboard cutting and metal pipe cutting are presented. Excitation force is computed by measuring the acceleration experienced by the reciprocating saw. Later these values are used as input to the E-model.

4.2.1 Free Run

Vibration measurement was carried out on reciprocating saw while running freely in air at two speed levels(Speed level-1 and Speed level-2). Further, in each speed level the reciprocating saw was tested at quarter speed, half speed and full speed. Note that the machine has only two speed levels and each speed level can be switched manually by shifting the speed pre-selection. Different speeds at each speed level were obtained by manually pressing the control switch on the tiger saw cf.Figure.4.1.

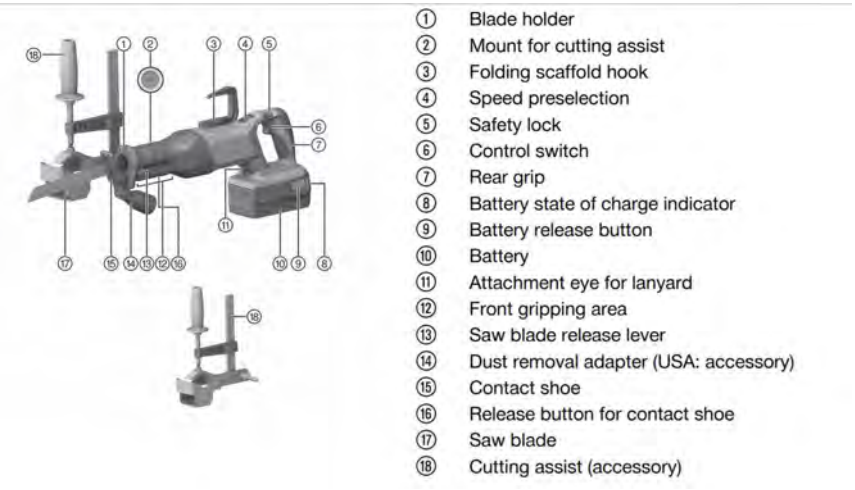

Figure 4.1: *Product Overview of Reciprocating Saw-SR-30A36 taken from Hilti Catalog, [22]*

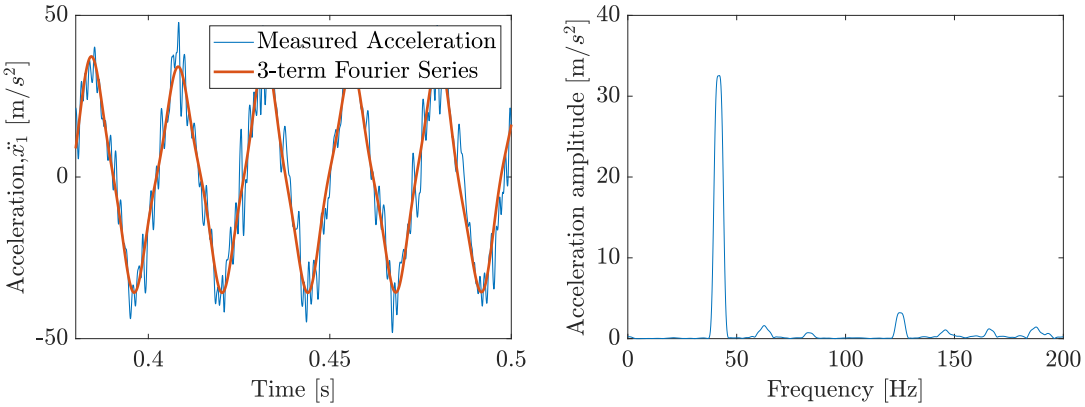

(a) *Measured acceleration signal fitted with 3 term Fourier Series*

(b) *FFT of measured Acceleration signal*

Figure 4.2: *Accelerations along cutting direction at full speed level-1 with free run condition*

The acceleration along the cutting direction and perpendicular direction is prominent due to the reciprocating motion of the blade and rotary motion of counter

balance in the rotor. Hence, measured acceleration signal along the cutting direction and perpendicular direction was analysed. The analysed data was fitted with a 3-term Fourier series for accelerations along cutting direction cf.Figure.4.2 and 4-term Fourier series for perpendicular direction to blade motion cf.Figure.4.3 after performing FFT of acceleration signals with flat-top window function.

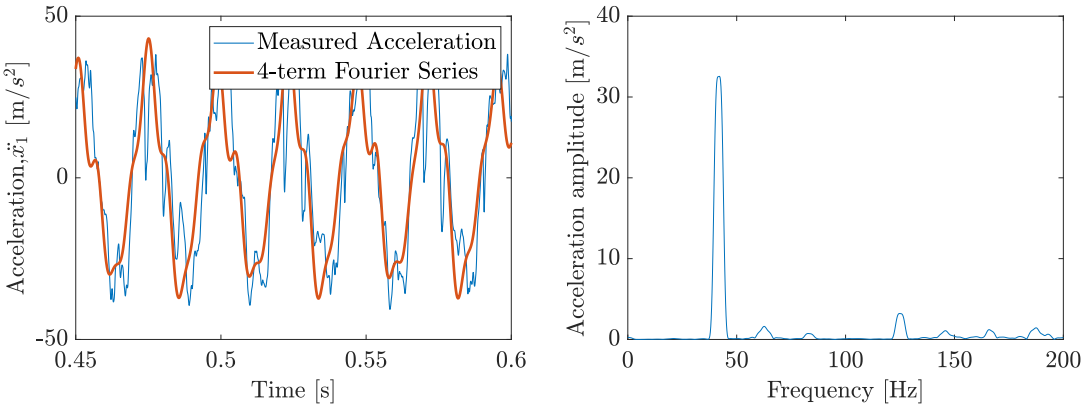

(a) *Measured acceleration signal fitted with 4 term Fourier Series*

(b) *FFT of measured Acceleration signal*

Figure 4.3: *Accelerations perpendicular to cutting direction at full speed level-1 with free run condition*

An equivalent acceleration amplitude is derived by considering a single harmonic wave at a reference frequency. The reference frequency is identified from the first peak in the FFT. Equivalent acceleration amplitude is computed by equating the absolute area (impulse) of the fitted fourier series with a sinusoidal wave at reference frequency. For the free run scenario, the equivalent acceleration amplitude was calculated as 32.7 m/s^2 in cutting direction and 31.5 m/s^2 in perpendicular direction at a reference frequency of 42 Hz. Similarly, equivalent acceleration was computed to speed level-2 and the set of results are presented in the Table.4.1

Along Cutting direction		
Speed Level	Acceleration Amplitude [m/s^2]	Frequency [Hz]
1	32.7	42
2	39.1	47
Perpendicular to Cutting direction		
Speed Level	Acceleration Amplitude [m/s^2]	Frequency [Hz]
1	31.5	42
2	37.2	47

Table 4.1: *Equivalent acceleration amplitude in free run*

Video Tracking

The vibrating motion of the reciprocating saw was filmed using the high speed camera and the video was analysed in the tracker software,cf.Figure.4.4. The results from the video tracking are presented here. Note that the reciprocating saw was hand held in horizontal position while video recording. The idea behind recording the data was to verify the time integration of acceleration signal to be able to find the vibration amplitude along blade movement while freely running the reciprocating saw. Later the vibration amplitude obtained from Video tracking is compared with double integration of acceleration data obtained by sensors.

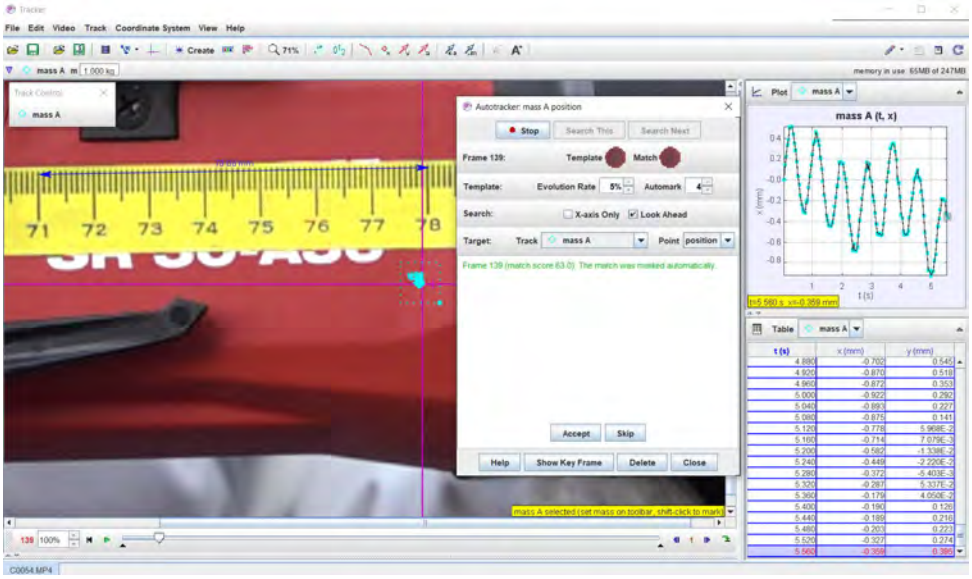

Figure 4.4: *Video Tracking of Reciprocating Saw using Tracker software*

Due to the presence of dynamic loads, it was impossible to hold the reciprocating saw in horizontal position while freely running. Hence there is random motion of the reciprocating saw which is not desirable in computing vibration amplitudes. To filter out undesired motion, primarily an auto tracker option along desired direction (*x-axis*) is used in *Tracker* software. The displacements obtained from *Tracker* software is analysed in Matlab. Firstly an FFT of the displacement data is made in Matlab using *fft* function. It is found that there are low frequency content and hence low frequency content (2 Hz) is removed from the displacement data to obtain the vibration amplitude.
The amplitude of vibration during free run is observed as 0.4 mm, c.f,Figure.4.5. Acceleration signal along cutting direction from Sensor-1 is used for double integration to obtain displacements for all times. Double integration was performed in MATLAB using *cumtrapz* function.

4.2.2 Chipboard Cut

Measurements of acceleration while cutting chipboard are recorded using 2 accelerometers and the measurement results are presented in this section. The cut

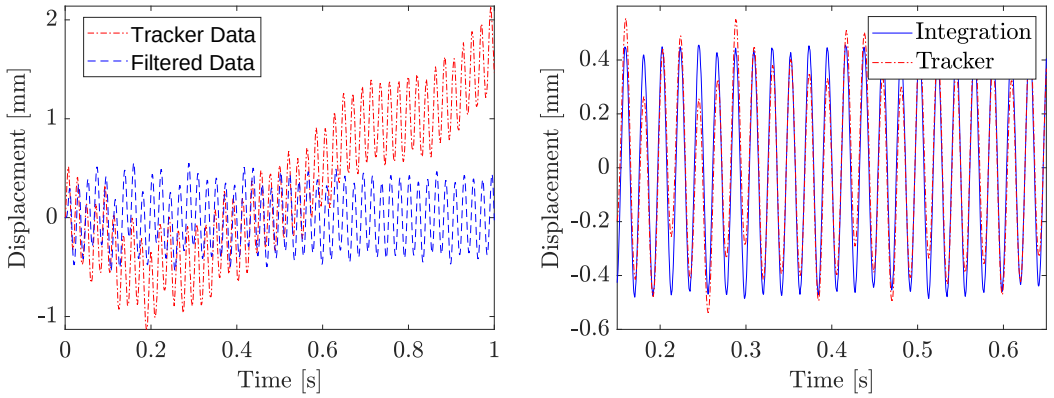

(a) *Tracker data at full speed level-2* **(b)** *Double Integration*

Figure 4.5: *Vibrations along cutting direction at full speed level-2 with free run condition*

was performed at speed levels 1 and 2. The cut was faster with speed level 2 in comparision with speed level 1. The fft of acceleration signal showed that the vibrations out of plane were insignificant. Hence the accelerations along the cutting direction are analysed. FFT of accelerations along cutting direction revealed 8 peaks and the time domain data was fitted with 8 term Fourier series, c.f.Figure.4.6. Equivalent acceleration is computed from the fitted fourier series as 51.1 m/s^2 at a reference frequency of 47 Hz.

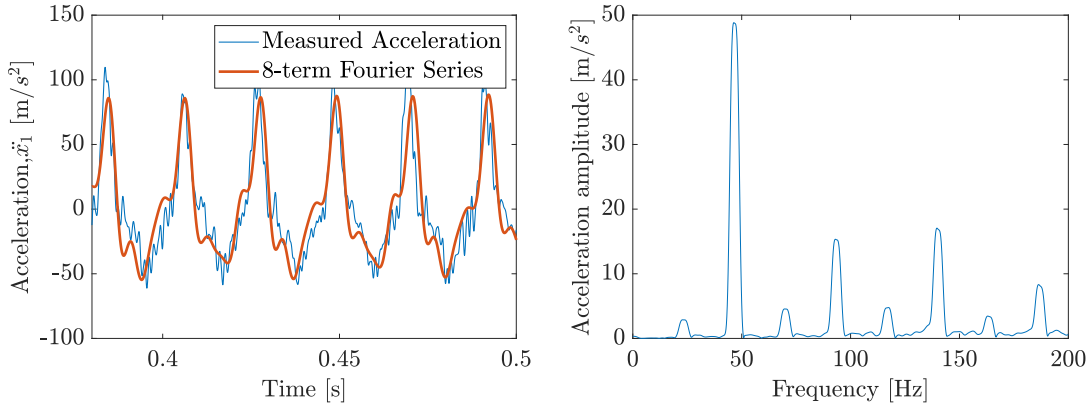

(a) *Measured acceleration signal fitted with 8 term Fourier Series* **(b)** *FFT of measured Acceleration signal*

Figure 4.6: *Accelerations along cutting direction at full speed level-2 while cutting chipboard in horizontal direction*

Amplitude of vibration is of interest and hence the acceleration signal,c.f.Figure.4.6a is double integrated and the amplitude of vibration is obtained as 0.5 mm in Speed level 1 and 0.6 mm in Speed level 2. Displacement obtained from both the sensor via double integration shows that the vibration close to blade is higher when compared to handle and can be observed in Figure.4.7.

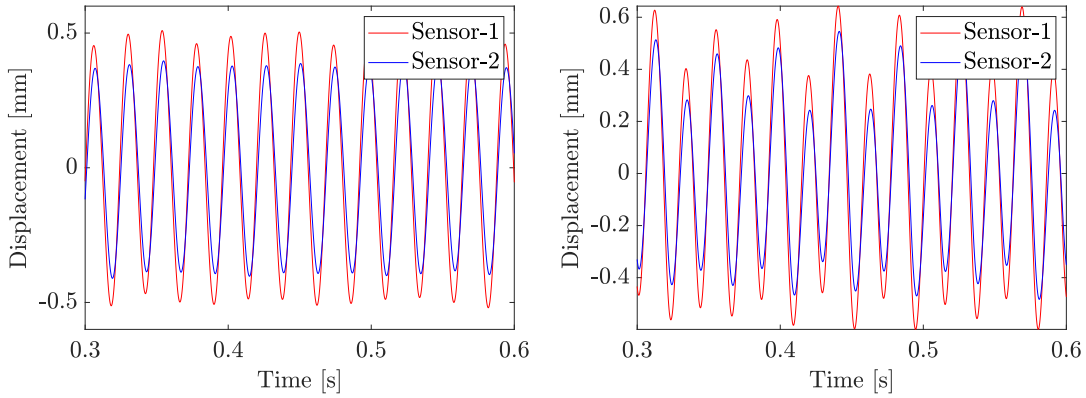

(a) *Speed Level-1* **(b)** *Speed Level-2*

Figure 4.7: *Double integration of acceleration along cutting direction while cutting chipboard*

4.2.3 Metal-pipe Cut

Metal cutting using reciprocating saw is done at speed level-1. Accelerations measured while cutting metal-pipe show very high peaks in comparision to free run and chipboard cut. This was expected since the cutting force generated while cutting metal is higher when compared to rest of the cases. Peak acceleration amplitude of $84\,\mathrm{m/s^2}$ was recorded at 42 Hz. The measured acceleration signal is fitted with a 5 term Fourier series, c.f.Figure.4.8. The fitted Fourier series resulted in an equivalent acceleration of $87.2\,\mathrm{m/s^2}$ at a reference frequency of 42 Hz.

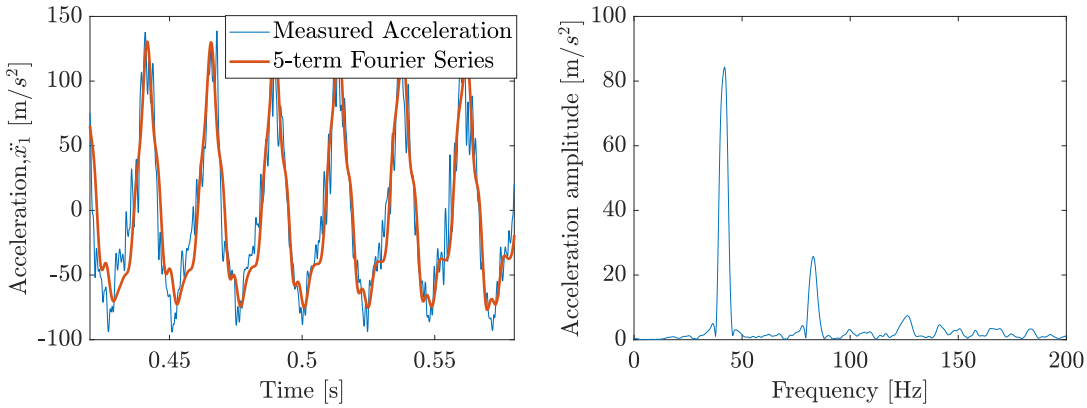

(a) *Measured acceleration signal fitted with 5 term Fourier Series* **(b)** *FFT of measured Acceleration signal*

Figure 4.8: *Accelerations along cutting direction at full speed level-1 while cutting metal-pipe*

Vibration amplitudes while cutting metal-pipe is computed in a similar way as it was done for previous case. The vibration amplitude was observed to be 1.1 mm in Sensor -1 and 0.8 mm in Sensor-2 ,c.f.Figure.4.9

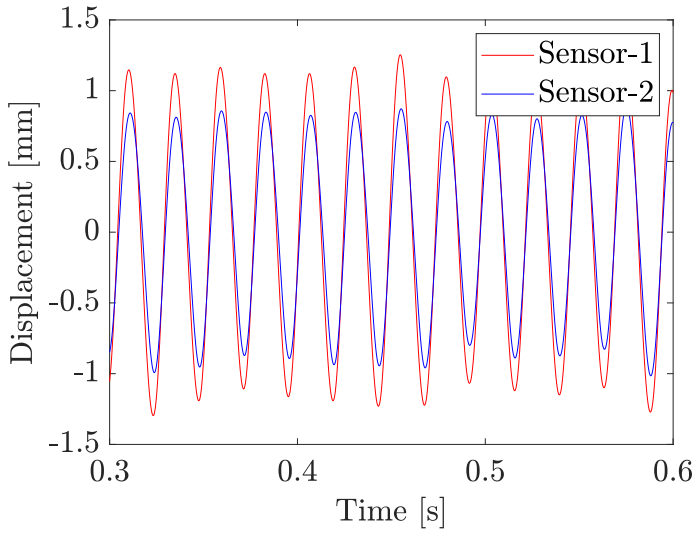

Figure 4.9: *Double integration of acceleration along cutting direction at Speed level-1 while cutting metal-pipe*

4.3 Excitation force amplitude

Input to the engineering model of the reciprocating saw is derived from the above measurement data. Two types of excitation forces are considered for the engineering model. The first one considers the mean of acceleration along the cutting direction from all the three scenarios and it is referred to as case-1 from here on wards. This case best represents the reciprocating saw with a counter-balance and ignores all the vibrations in perpendicular direction. The reciprocating saw which was tested had an eccentric mass on the rotor to reduce vibrations along cutting direction. The eccentric mass on the rotor generates vibration perpendicular to cutting direction,c.f.Figure.4.3. In the second case, an equivalent acceleration is assumed by considering a situation wherein there is no eccentric mass on the rotor, since measurements without eccentric mass on the rotor was not possible. Acceleration amplitude in second case is the sum of average acceleration amplitude from case-1 and average acceleration from perpendicular direction (both Speed level-1 and Speed level-2) in free run. Note in both the cases the acceleration values corresponds to an equivalent acceleration amplitude obtained by equating the absolute area under fitted Fourier series with a harmonic wave at a reference frequency. The preliminary idea was to to solve the problem for case-1. Based on the results from case-1, case-2 will be considered for further analysis or future work.

Excitation force amplitude acting on the reciprocating saw is very much dependent on frequency. During free run measurements it was observed that the acceleration amplitude vary quadraticaly with frequency,cf.Figure.4.10. One can expect this result since the acceleration in a slider crank mechanism depends on ω^2, refer the acceleration expression for slider crank mechanism given in Appendix A. Thus the input to the engineering model for case-1 is defined by Equation.4.1 [7],[8] wherein

the reference acceleration a_{ref} is obtained as average acceleration amplitude at a reference frequency given in Table.4.2. Similarly in case-2 the reference acceleration amplitude is computed to be as 86.9 m/s^2 at a reference frequency of 44.5 Hz. Note that case-2 is a hypothetical case and one can trust these values after conducting the acceleration measurements without eccentric mass on the rotor. Thus the optimization of the system parameters are conducted for case-1 only.

$$F_{e,RS} = F_{e,ref}\left(\frac{f}{f_{ref}}\right)^2 sin(2\pi ft)$$
$$F_{e,ref} = m_m a_{e,ref} \tag{4.1}$$

In above Equation.4.1, the reference force is computed based on equivalent reference acceleration amplitude given in Table.4.2 and the mass of reciprocating saw (m_m).

Case-1		
Scenario	Acceleration Amplitude [m/s^2]	Frequency [Hz]
Free Run-1	32.7	42
Free Run-2	39.1	47
Chipboard Cut	51.1	47
Metalpipe Cut	87.2	42
Average ($a_{e,ref}$)	52.5	44.5

Table 4.2: Equivalent acceleration amplitude along cutting direction from measurements

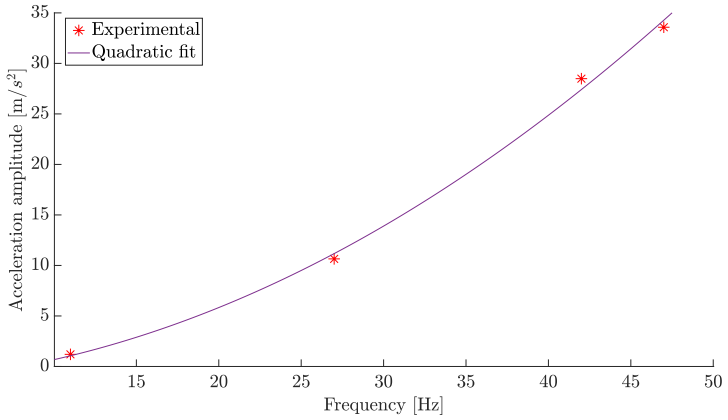

Figure 4.10: *Measured Acceleration amplitude at free run*

4.4 Parameter Sensitivity

The engineering model for the reciprocating saw is defined by set of parameters such as stiffness and mass properties. The stiffness and mass properties of the non-linear system influence the vibration supression. It is very important to make an engineering guess which defines the parameter values and one has to have an idea of how the parameter influence the response of the system. The parameters listed in Table.3.1 is used as arbitrary set and single parameter is varied at a time to understand the sensitivity of respective parameter. The sensitivity of parameters will guide in selecting realistic bounds for optimization of parameters.

Stiffness and Damping at work-piece interface

In the engineering model, a linear spring and damper is assumed between the reciprocating saw and the work-piece. In reality, there are no mechanical springs between reciprocating saw and work-piece. The interaction of reciprocating saw and work-piece is assumed by a linear spring and damper. This is an engineering assumption and by varying this parameter one can understand how much influence it has on the frequency response of main mass, cf.Figure.4.11. The RMS of main mass displacement is computed for each frequency step as given in Equation.4.2.

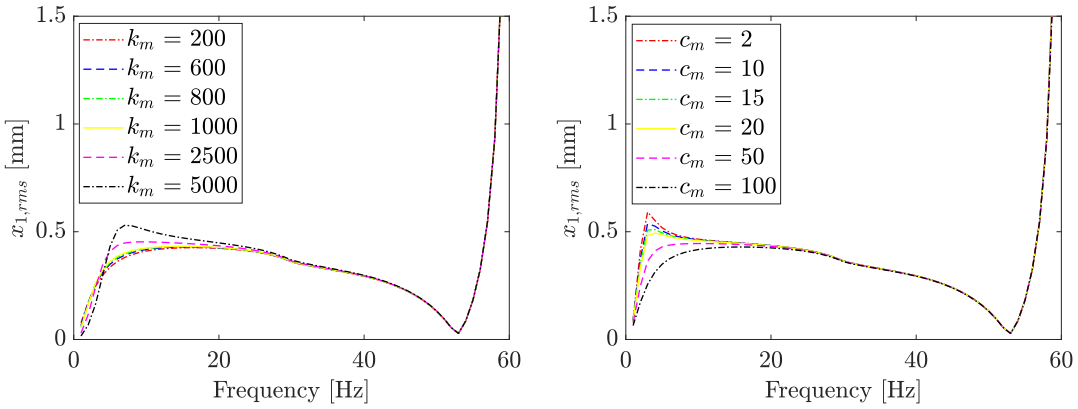

(a) *Main mass response for different values of* k_m[N/m]

(b) *Main mass response for different values of* c_m[Ns/m]

Figure 4.11: *Main mass response for different stiffness and damping properties at work-piece interface*

$$x_{1,rms} = \sqrt{\frac{1}{N}\sum_{i=1}^{N} x_i^2} \tag{4.2}$$

It can be observed that different values of k_m, c_m have no influence on main mass response after 30 Hz. The ground stiffness value influences the first resonance frequency and the damping effects the peak response at first resonance frequency. To keep the the first resonance value to be around 8 Hz and peak rms response to be as low as possible, a moderate stiffness of 600 N/m and high damping of 100 Ns/m

is selected for further analysis. These values were also used in the previous work [8] to check ATVA feasibility for reciprocating saw application.

Stiffness and Damping at operator interface

The human interaction with the machine is also modelled as linear spring and a viscous damper in the engineering model. The stiffness and damping value has very little influence on the overall response. Stiffness, damping values to be used was suggested in previous thesis work [7] as $k_p = 1000\,\mathrm{N/m}, c_p = 60\,\mathrm{Ns/m}$. The sensitivity of these 2 parameters are exactly similar to k_m, c_m, cf.Figure.4.12 and can be realized by looking at the equations of motion (Equation.3.2) of the non-linear system. Hence the values suggested in [7] are adopted in this thesis work also.

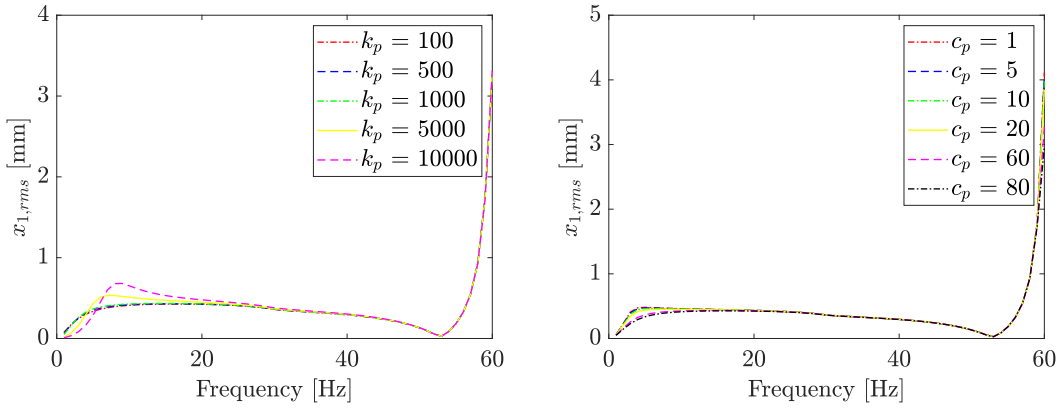

(a) *Main mass response for different values of* k_p[N/m]

(b) *Main mass response for different values of* c_p[Ns/m]

Figure 4.12: *Main mass response for different values of stiffness and damping at operator interface*

Damping between main mass and Auxiliary mass

For a tuned absorber to be effective the damping value should be kept as low as possible. Low damping values will influence the vibration suppression over wide range of frequencies. Since the goal is to keep the anti-resonance frequency range wide and still be able to get sufficient vibration suppression, a damping value of $c_a = 1\,\mathrm{Ns/m}$ was assumed in [7],[8]. This assumption has great influence on the vibration attenuation and one has to verify the actual damping experimentally. Note that in this thesis work the damping between main mass and auxiliary mass is not experimentally estimated instead the damping coefficient c_a is assumed to be 1 Ns/m. The model response for different damping values are shown in Figure.4.13. It was observed that for a lower damping value of 1 Ns/m the main mass has lowest rms response at anti-resonance point whereas for higher damping coefficient say 20 Ns/m the main mass rms response is at least 15 times higher when compared to low damping. This suggests that the ATVA is highly sensitive to damping.

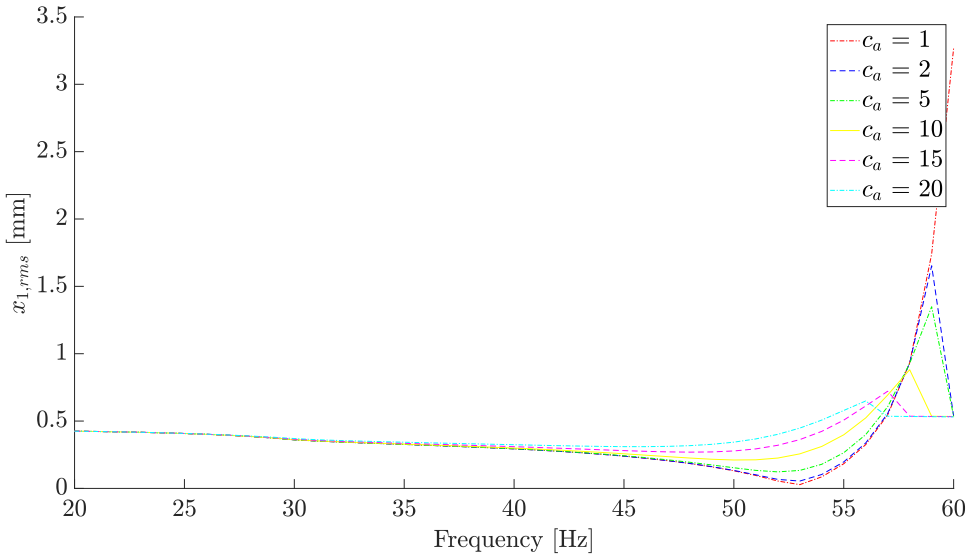

Figure 4.13: *Main mass response for different values of* c_a[N/m]

Soft Spring-k_1

The soft spring k_1 plays vital role in activating ATVA. Auxiliarry mass (m_a) is always actively moving because of the soft spring. So the stiffness parameter k_1 is varied while all other parameters are set as given in Table.3.1. It is of interest to study the frequency response of the non-linear system for different k_1 values and it is shown in Figure.4.14

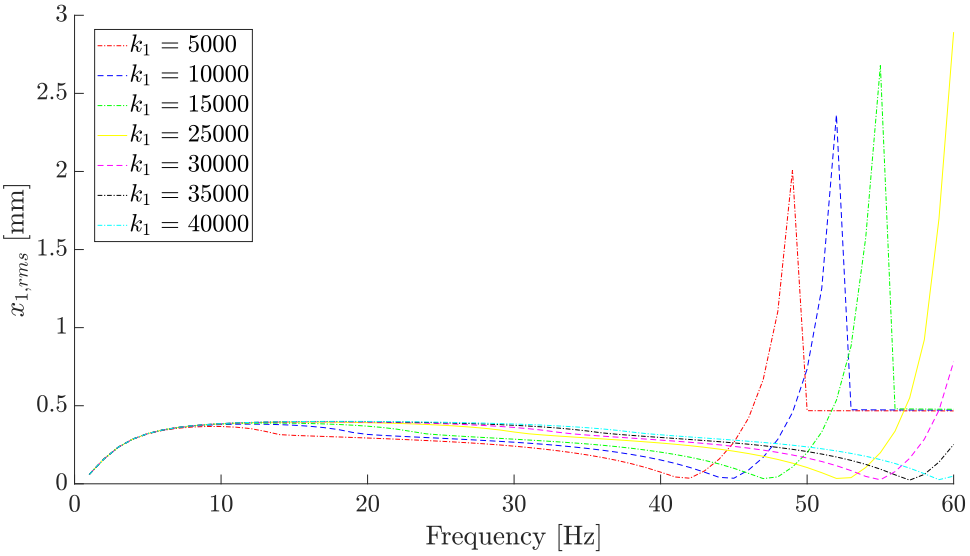

Figure 4.14: *Main mass response for different values of* k_1[N/m]

It can be observed that the increase in stiffness values, results in shifting the resonance towards right. The same trend can also be observed for the anti-resonance points. The peak rms values increase with increase in resonance frequency. Fre-

quency response of main mass shows broadened anti-resonance points for k_1 = [5,10,15,25] $\times$ 10^3 N/m, whereas for higher stiffness the response curves widens more since the second resonance frequency increases with k_1.

Hard Spring-k_2

Hard spring constitutes the secondary stiffness in the ATVA. The action of hard spring with stiffness k_2 is highly influenced by the gap α. Frequency response of main mass is studied for different values of k_2, cf.Figure.4.15

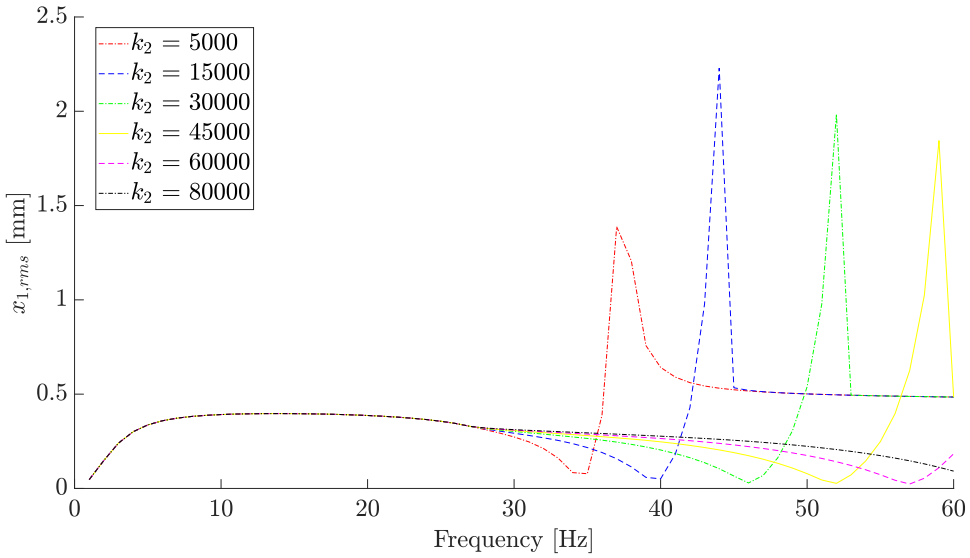

Figure 4.15: *Main mass response for different values of* k_2[N/m]

By varying k_2 stiffness, it is observed that the increase in stiffness results an increased resonance frequency similar to varying k_1. The anti-resonance points move farther as k_2 value increases which is also similar to k_1.The secondary stiffness plays major role in broadening the anti-resonance point. Smaller stiffness values of $k_2 = [5000, 15000]$ N/m has less broadening when compared to $k_2 = [30000, 45000, 60000]$N/m.

Gap-α

The non-linearity in stiffness is induced with the parameter α. The gap between soft and hard spring makes the frequency response broaden at anti-resonance point, cf.Figure.4.16.

By increasing the gap between soft and hard spring the vibrations in main mass is suppressed for an increased range of excitation frequency. For instance, with smaller gap length ($\alpha = 0.2\,\text{mm}$) the entire system works mostly as a linear tuned vibration absorber whose tuned frequency is slightly less than $\sqrt{\frac{k_1 + k_2}{m_a}}$. With gradual increase in the gap the anti-resonance point broadens across different central points. The central point refers to the lowest rms value achieved for any given gap.

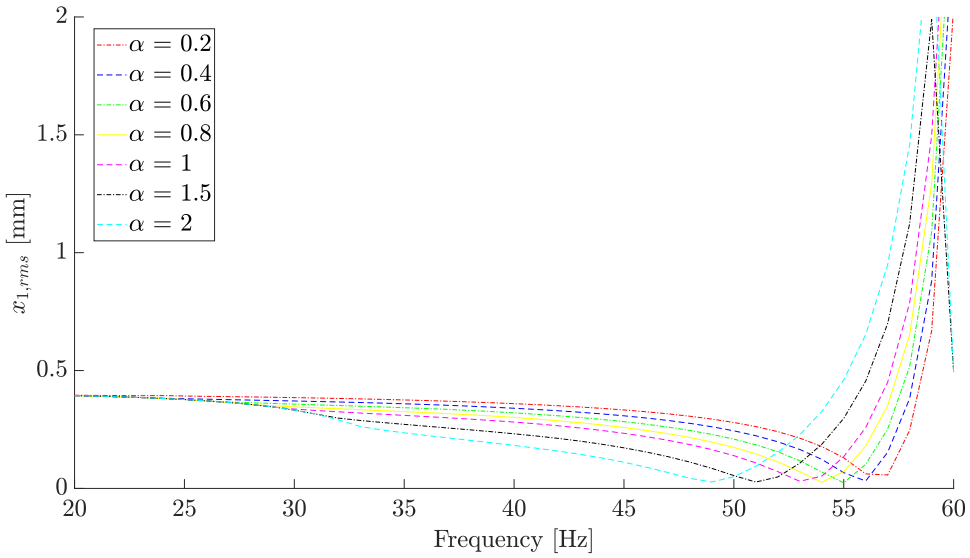

Figure 4.16: *Main mass response for different values of* α[mm]

Reference Force

The reference force influences the resonance and anti-resonance points because of the non-linear spring stiffness and it can be observed in Figure.4.17. With the increase in load, the vibration suppression band reduces. This means to say that the system approaches to linear region. The gap α determines the load at which the system shifts towards linear region. This sets up limitation on ATVA. So for an optimum performance of ATVA the system parameters k_1, k_2, α has to be tuned for a known input force with knowledge of input force and excitation frequency variation.

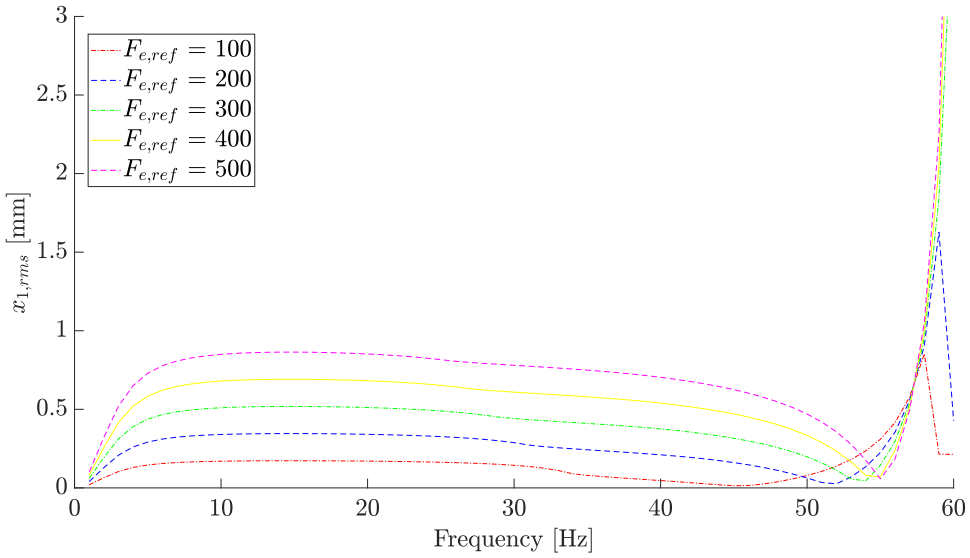

Figure 4.17: *Main mass response for different values of* $F_{e,ref}$[N]

4.5 Model Validation

The engineering model response is computed for different inputs as obtained from measurements (Table.4.2). This ensures that the engineering model is fair enough in representing the reciprocating saw in practical applications. The engineering model considered for model validation is shown in Figure.4.18 for three different scenarios. The actual vibration amplitude from the measurements is compared against the model response for all three measurement scenarios.

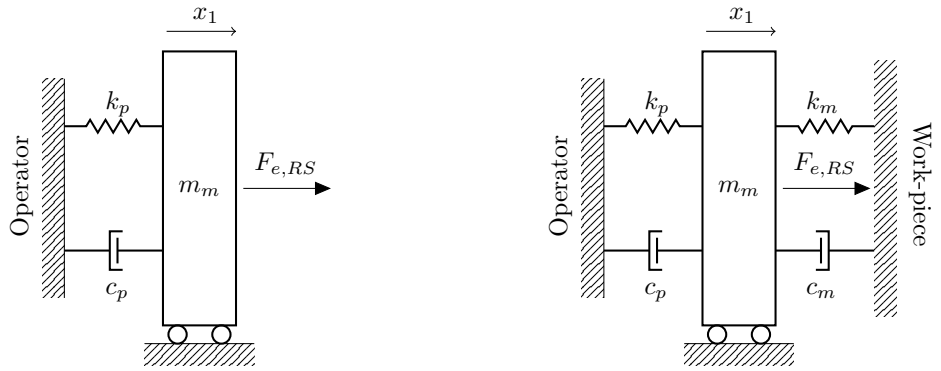

(a) *Free Run* **(b)** *Chipboard/Metal-pipe Cut*

Figure 4.18: *Engineering model of Reciprocating saw during Measurements*

Input to the E-model is the excitation force ($F_{e,RS}$) described in Equation.4.1 and the reference excitation frequency is considered to be as $f_{ref} = 45\,\text{Hz}$. Equations of motion for the above E-models are given in Equation.4.3 and Equation.4.4. The main mass(m_m) is the mass of the reciprocating saw and was measured to be as 4.4 kg and other stiffness and damping parameter values are listed in Table.4.3. The stiffness and damping properties was chosen by looking at the model response during parameter sensitivity check. Also the parameter values related to operator stiffness and damping are chosen based on previous work done at RISE [7],[8].

Parameter	Value
m_m	4.4 kg
k_m	600 N/m
k_p	1000 N/m
c_m	100 Ns/m
c_p	60 Ns/m

Table 4.3: System Parameters used for validation

Free Run

$$m_m\ddot{x_1} + c_p\dot{x_1} + k_p x_1 = F_{e,RS} \tag{4.3}$$

In Equation.4.3 the input force is $F_{e,RS}$ and it represents the excitation force in the machine caused due to reciprocating motion.The magnitude of force is obtained from Table.4.2 by multiplying the acceleration amplitude with main mass. This input excitation force is considered along the cutting action only. The engineering model response for free run and the measurement data obtained by tracking a point on reciprocating saw agree each other,cf.Figure.4.19

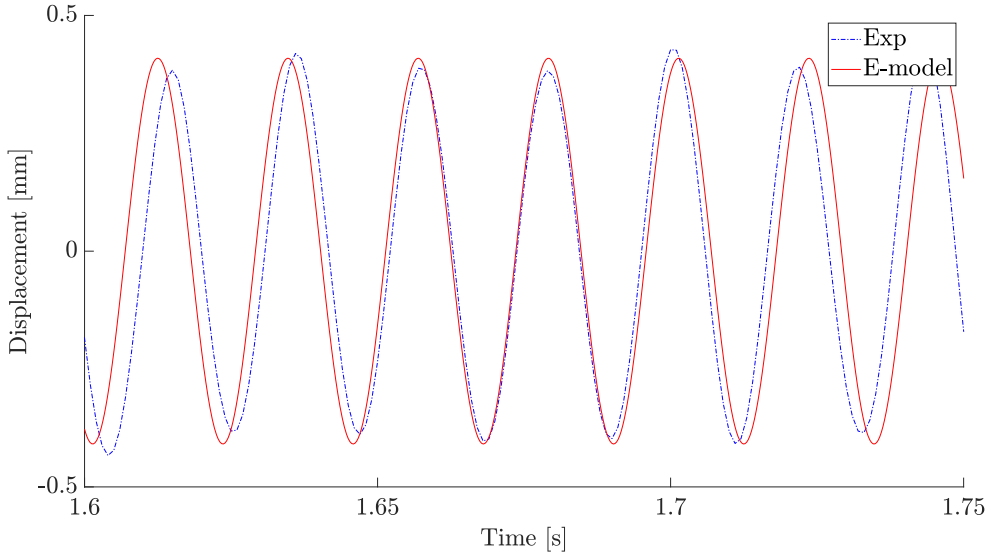

Figure 4.19: *Model Validation of Engineering model during free run condition at speed level-2*

Peak displacement amplitude obtained from engineering model is 0.4 mm whereas the peak amplitude obtained from experiment is 0.38 mm. Thus a marginal difference of 0.02 mm is observed accounting to an error of 5.26%.

Chipboard/Metal-pipe Cut

$$m_m\ddot{x_1} + (c_p + c_m)\dot{x_1} + (k_p + k_m)x_1 = F_{e,RS} \tag{4.4}$$

In Equation.4.4 the input force represents the unbalance force and cutting force generated during cutting action. The direction of $F_{e,RS}$ is along the reciprocating action only. The engineering response for chipboard cutting and metal pipe cutting is compared with the actual measurements in the Figure.4.20. It can be observed that the engineering model of reciprocating saw with measured input force predicts the response with an error of 5%.

Generalized Input

Reciprocating saw work for a wide range of excitation forces and it can be observed from the measurement results for different cases. Hence a generalized reference force

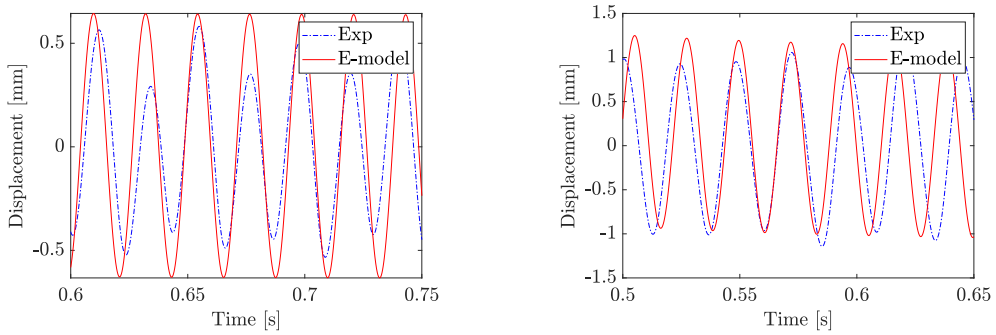

(a) *Chipboard Cut* **(b)** *Metal-pipe Cut*

Figure 4.20: *Model Validation of Engineering model during cutting*

is obtained from all three sceanrios by taking average of measured acceleration amplitudes and such a force is called as reference force. The E-model response for reference force input is shown in Figure.4.21 and is compared with actual measurements.

The decided reference force of magnitude 231 N predicts a moderate response which has higher amplitudes when compared to free run and chipboard cut. But predicts slightly lower peak amplitudes for metal cutting. Hence, the E-model with reference force is considered to be a general case and the ATVA is optimized for this reference input force.

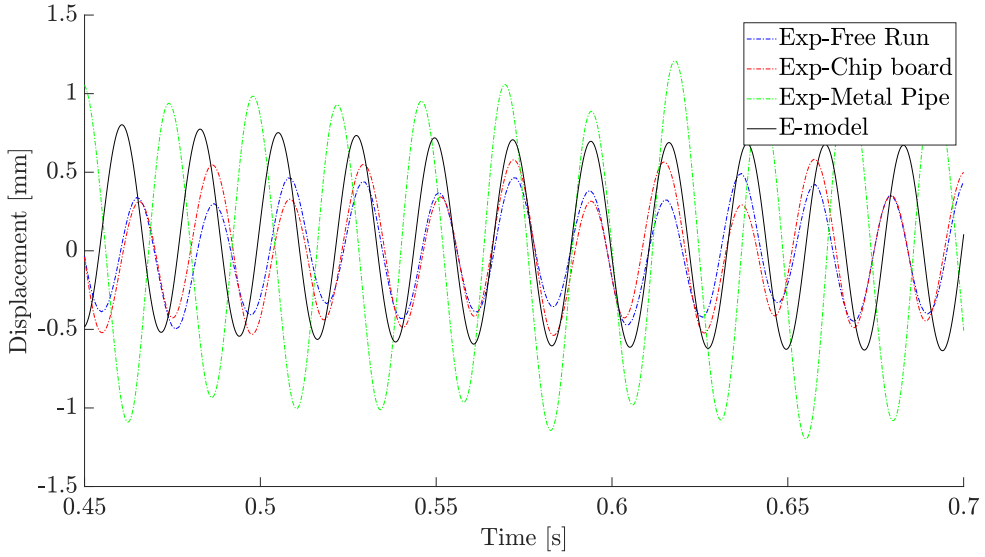

Figure 4.21: *Model response of engineering model at Reference Force*

5
Optimization

This chapter deals with optimization of mass and stiffness properties of non-linear auxiliary system. A brief description of the objective function used for the optimization and the method followed to construct the objective function is given. Finally, the optimization results are presented.

5.1 Non-Linear Optimization

ATVA behaviour depends on the spring stiffness k_1, k_2, α and the auxiliary mass m_a. The number of parameters to optimize is 4 and those are called as free parameters. All other stiffness and mass properties are fixed to the values given in Table.4.3. The vector of 4 parameters is called as (P), Equation.5.1.

$$P = \begin{bmatrix} k_1 & k_2 & \alpha & m_a \end{bmatrix} \tag{5.1}$$

$$P = P_0 \times (p + 1) \tag{5.2}$$

The optimization of the parameters should have realistic upper and lower bounds. Selection of bounds was made by doing trial optimizations. The start points for optimization was randomly chosen within the bounds by defining a normalized parameter (p) and initial parameter (P_0), refer Equation.5.2,[7]. Normalized parameter(p) was obtained by considering the upper and lower limits(*rand* function in matlab was used). In this thesis work, ATVA is optimized for the reference input force which was measured in the presence of eccentric mass on the rotor of reciprocating saw. The optimization of these 4 free parameters are taken in 3 steps. The first step involves optimization of all 4 free parameters at a time. The second optimization is done by fixing the ATVA mass as fixed parameter. In third step, based on results from step-2 a suitable and available spring stiffness is selected from spring catalog,[12]. The selected spring stiffness from catalog is made to be fixed parameter and the the gap(α) is optimized in the final optimization. Later with these results the prototype of ATVA is constructed.

5.1.1 Objective Function

The objective function,L evaluates the performance of the absorber. One would expect the absorber is effective in reducing vibration levels while adopting itself for a wide range of excitation frequency. In the previous thesis work performed at RISE, a similar objective function was constructed to perform optimization of absorber for

pneumatic breaker application, [7]. The objective function to be used in this thesis work is built based on the previous work.
Objective function,L should consider response of absorber over a range of excitation frequencies. The range of excitation frequency is decided based on the measurement results. The measurements showed that the reciprocating saw operates from 42 Hz to 47 Hz. With the range known, a central frequency to the range is selected and it is called as mean tuning frequency (f_{nom}). In this case the mean tuning frequency accounts to 45 Hz. It was decided to use ± 10 % variation from mean tuning frequency. Hence the frequency range of interest is given by Equation5.3.

$$f \in [f_{lb}, f_{ub}] = [0.9 f_{nom}, 1.1 f_{nom}] \tag{5.3}$$

The response at each excitation frequency has to be weighed for the optimized parameters to be robust. The weighting function considers normal distribution of the frequency and is defined by Equation.5.4, [7].

$$W(f) = \mathcal{N}\left(f_{\text{nom}}, \sigma^2\right) = \frac{1}{\sigma\sqrt{2\pi}} e^{-\frac{(f-f_{\text{nom}})^2}{2\sigma^2}} \tag{5.4}$$

The standard deviation σ is defined based on weighting function (Equation.5.4) and the frequency band considered in Equation.5.3. Further it was decided that weights at first and last frequency points be 1/3 of the weight at nominal frequency, [7].

$$\sigma = \sqrt{\frac{(0.10 f_{\text{nom}})^2}{-2\ln(1/3)}} \tag{5.5}$$

The objective function is greatly influenced by the frequency band and the weights. Both these values are estimations. The important fact is that the ATVA should suppress vibrations at mean tuning frequency and ATVA performance should not be drastically affected within the defined range of excitation frequency (±10%).

Instead of multiplying the weight function with the response at each equidistant frequency step, non-equidistant frequency steps was defined which is inversly proportional to the weights at particular frequency. Formulation of non-equidistant frequency steps using the weight function was adopted from [7]. The frequency range considered with unequal spacing is used for defining the objective function, L with the normalized parameter set p as follows, refer Equation.5.6. Note: Objective function L in Equation.5.6 contains sum of velocity rms response of main mass at different discretized frequencies within ±10% of mean tuning frequency.

$$L(p) = \frac{1}{2} \sum_{i=1}^{N-1} \left(\dot{x}_{1,\text{RMS}}\left(f_i, p\right) + \dot{x}_{1,\text{RMS}}\left(f_{i+1}, p\right) \right) \tag{5.6}$$

Later, the non-linear least squares formulation is made as given in Equation.5.7. This formulation of objective function is subjected to minimization in Matlab using *lsqnonlin*. The objective function used here and implemented in Matlab outputs vector values as given by Equation.5.6. *lsqnonlin* computes the norm of the objective function and hence the formulation looks as given in Equation.5.7 wherein Equation.5.8 is similar to Equation.5.6.

$$\begin{aligned} l_i(p) &= \sqrt{\dot{x}_{1,\mathrm{RMS}}\left(f_i, p\right)}, \quad i = 2, \ldots, N-1 \\ l_i(p) &= \sqrt{\frac{1}{2}\dot{x}_{1,\mathrm{RMS}}\left(f_i, p\right)}, \quad i = 1, N \end{aligned} \tag{5.7}$$

$$L(p) = \sum_{i=1}^{N} l_i^2(p) \tag{5.8}$$

The Matlab function *lsqnonlin* incorporates the trust region reflective method with upper and lower parameter bounds. Parallel computation in Matlab is used for solving the minimization problem while simultaneously starting from random start points within the bounds to reach global minimum of the objective function. All computations were performed at Chalmers Cluster. Further, response from optimized parameters are compared against LTVA tuned at mean tuning frequency ($f_{nom} = 45\,\mathrm{Hz}$).

5.1.2 Optimization Results

Optimization of 4 parameters is first carried out with same bounds on k_1 and k_2. The upper and lower bounds used for the optimization are reported below in Table.5.1. The initial value (P_0) in the table refers to the parameter values which are used for obtaining random start points within the parameter bounds.

	k_1	k_2	α	ma
Lower Bound	1500 N/m	1500 N/m	0.1 mm	0.1 kg
Upper Bound	75 000 N/m	75 000 N/m	4.5 mm	0.5 kg
Initial Value (P_0)	15 000 N/m	40 000 N/m	1.8 mm	0.5 kg

Table 5.1: *Parameter Bounds*

In the first step of optimization, 792 random start points were used to identify the minimum objective function value. The objective function value resulting from different random start points are arranged in decreasing order, cf. Figure.5.1. The right most point in the plot represents the optimized objective function value. Optimization results of each parameter for all start points are arranged in descending order as shown in Figure.5.2. Soft spring with stiffness k_1 attains a stable value after 600 runs and thus shows that the parameter has influenced the objective function in attaining global minima. Unlike soft spring the hard spring with stiffness k_2 and the gap α attains values close to its upper bounds. This shows that increasing the bounds of k_2,α might result in a lower objective function value. Increasing the bounds on k_2 may not be a good option because of the unavailability of springs with high stiffness whose size is comparable to previous prototype. Further, some relaxation on upper bound can be given on the gap length (α) to see possibility of further reduction in objective function. It was observed that the auxiliary mass attains the upper bound value and it was expected since more mass results in increased counteracting force to the excitation force. Hence, parameter m_a is fixed to upper bound.

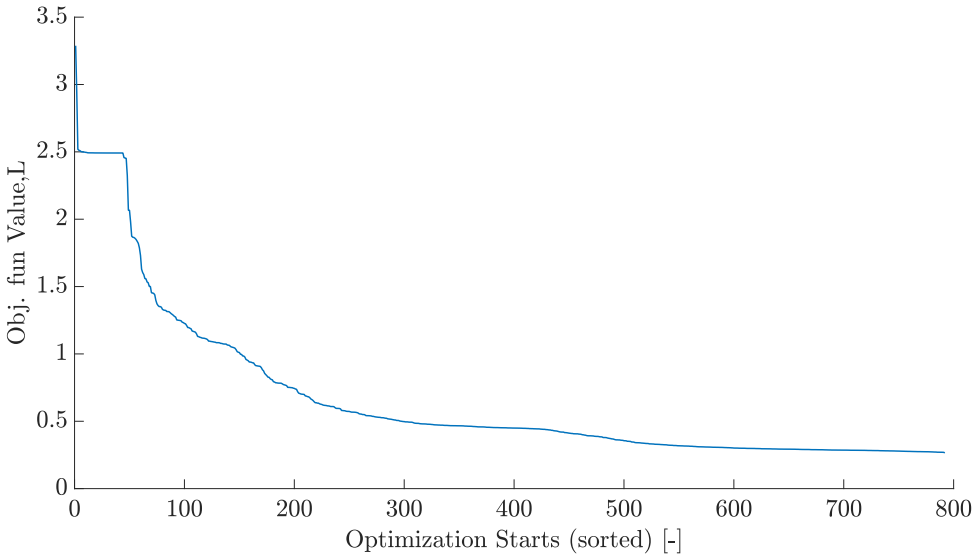

Figure 5.1: *Objective Function L for 792 different start points*

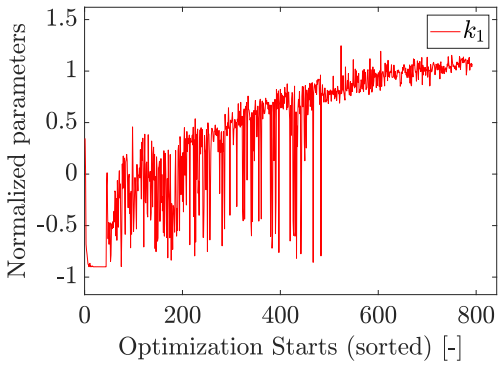

(a) *Optimization of parameter-k_1*

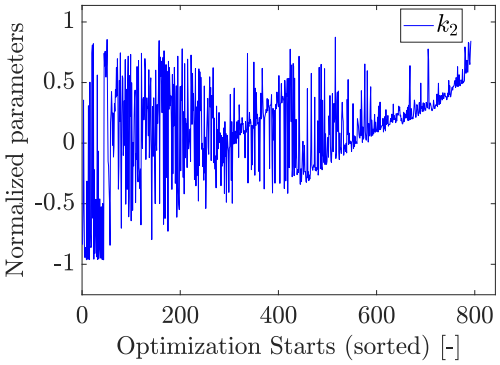

(b) *Optimization of parameter-k_2*

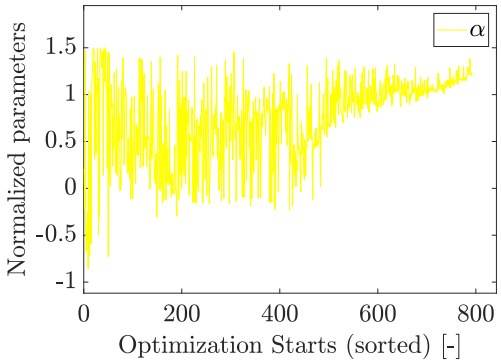

(c) *Optimization of parameter-α*

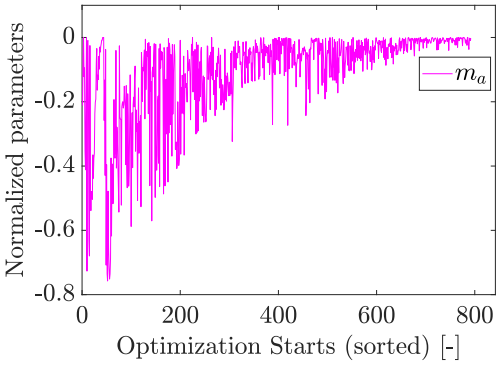

(d) *Optimization of parameter-m_a*

Figure 5.2: *Optimization results of 4 normalized parameters from 792 random start points*

Auxiliary mass cannot be made bigger than 0.5 kg due to practical limitations on placement of ATVA in the reciprocating saw. Also increasing mass would make the reciprocating saw heavy and thus making it difficult to handle. From first optimization, lowest objective function value of 0.2656 was attained after solving the minimization problem with the constraints defined in Table.5.1. The best parameter set which corresponds to minimum objective function value is $k_1 = 3.1052 \times 10^4$ N/m, $k_2 = 7.3760 \times 10^4$ N/m, $\alpha = 4$ mm, $m_a = 0.4985$ kg.
These results from first optimization is used to decide bounds on the stiffness in the second optimization. In the second optimization, the upper bound on k_1 is reduced to 50 000 N/m while lower bound on k_2 is increased to 40 000 N/m and the auxiliary mass is fixed to upper bound ($m_a = 0.5$ kg). As discussed above, the upper bound on the gap (α) is increased to 6 mm, while the lower bound was increased to 2 mm. The second optimization of three parameters is carried out in a similar fashion as that of first optimization and the objective function for 800 random start points is shown in Figure.5.3.

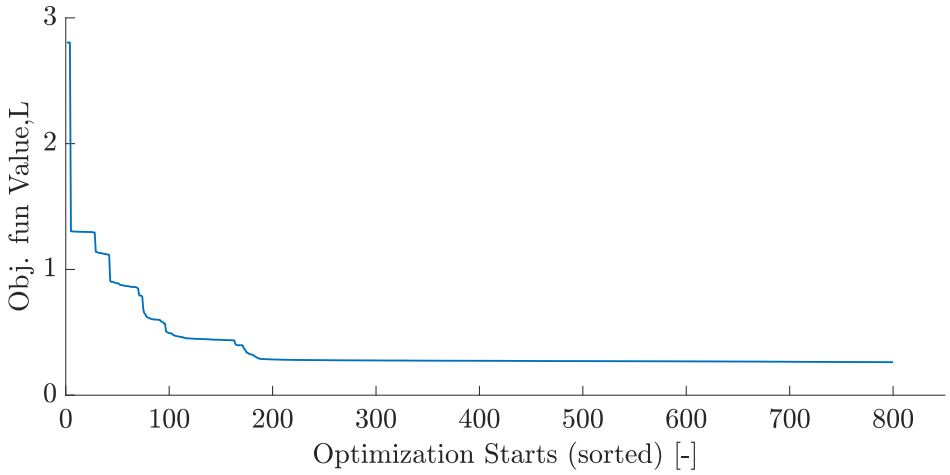

Figure 5.3: *Objective Function L for 800 different start points*

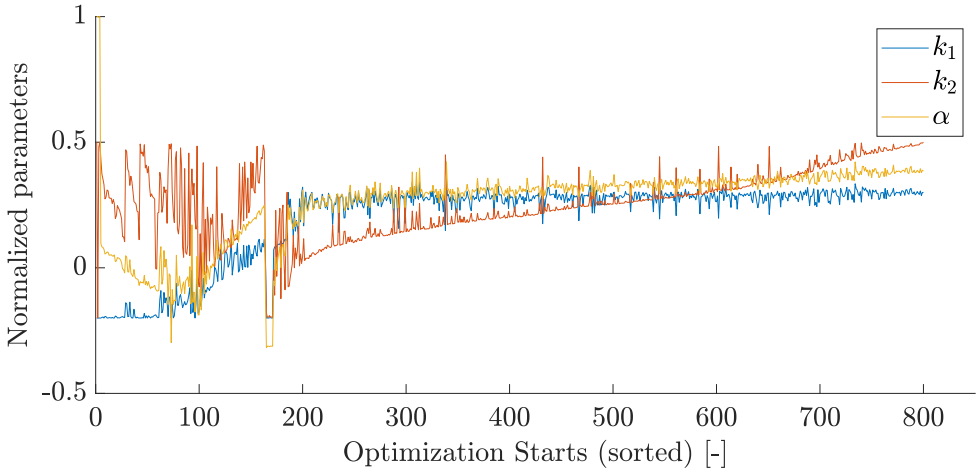

Figure 5.4: *Optimization of parameters-k_1,k_2,α*

In Figure.5.3 the objective function values L are arranged in descending order and the right extreme point shows the lowest value. Least value of L was found to be 0.2624. From the second optimization of parameters, it was observed that the parameters α, k_1 attains steady values for different start points even when their constraints are narrowed down when compared to first optimization, cf,Figure.5.4. This indicates that k_1 and α have reached optimum values. But the hard spring stiffness reaches the upper bound value as it was seen in the first optimization.

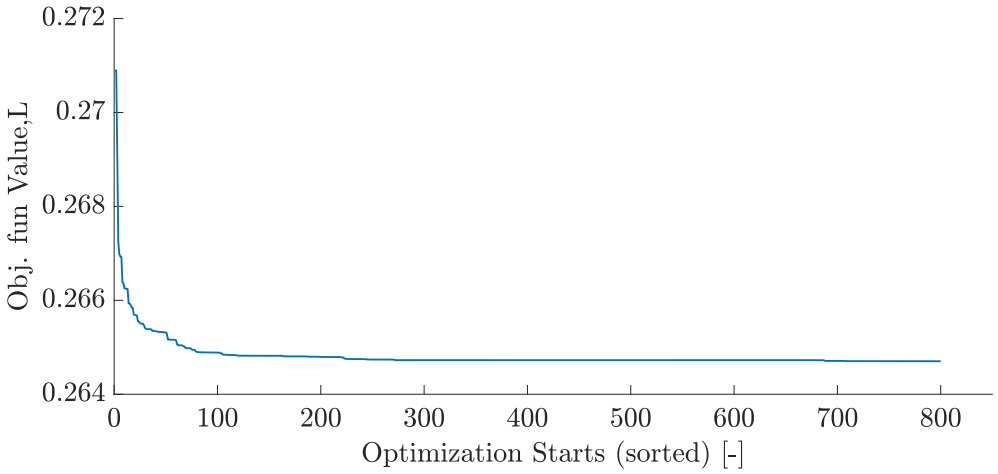

Figure 5.5: *Objective Function L for 800 different start points when k_1, k_2 are fixed*

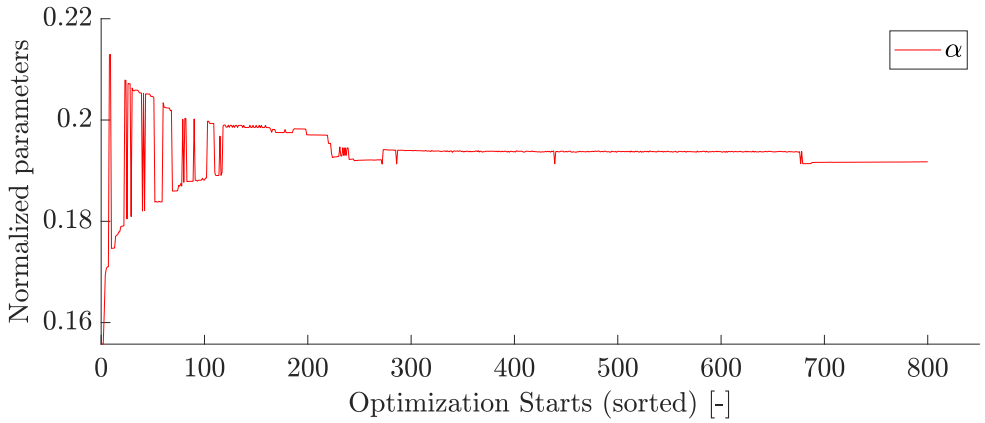

Figure 5.6: *Optimization of parameter α, while k_1, k_2 are fixed*

The upper bound on k_2 theoretically can be increased to obtain a lower objective function value provided such high stiffness spring should be practically possible. It was decided to increase the upper bound value of k_2 to 100 kN/m while the lower bound was set to 70 kN/m. The lowest objective function value for increased bounds on k_2 was found to be 0.2522, and k_2 reached upper limit. When compared to the previous optimization, the gain from increasing k_2 is 4% reduction in objective function. Theoretically, it suggests that stiffer the spring better the performance.

It also means that the stiffer spring would push the second resonance frequency farther away from the operating frequency. Hence, with the practical considerations the spring stiffness k_2 was set to 72.1 kN/m and k_1 was set to 33 kN/m. These stiffness values are chosen based on optimization results and springs available from spring catalog(Lesjöfors) [12].
A final optimization to find optimum gap (α) is done by fixing stiffness(k_1,k_2). Lowest objective function value of 0.2647 was obtained. The objective function values for 800 different start points is shown in Figure.5.5 and the optimization of gap α is shown in Figure.5.6. Table.5.2 shows the aggregate of optimization results. The last optimization result shown in the Table.5.2 are the final parameters for ATVA (Run -III). Prototype of ATVA is developed based on the final optimization result(Run-III). Appendix C shows the ATVA prototype construction.

Run	Parameter	Units	Status	Bounds		Optimum	Min Obj.fn,L
				Lower	Upper		
I	k_1	N/m	Free	1500	75000	31052	0.2656
	k_2	N/m	Free	1500	75000	73760	
	α	mm	Free	0.1	4.5	4	
	m_a	kg	Free	0.1	0.5	0.4985	
II	k_1	N/m	Free	20000	50000	32477	0.2624
	k_2	N/m	Free	40000	75000	74984	
	α	mm	Free	2	6	4.1	
	m_a	kg	Fixed	0.5		0.5	
II a	k_1	N/m	Free	20000	50000	32874	0.2522
	k_2	N/m	Free	70000	100000	99688	
	α	mm	Free	2	6	4.4	
	m_a	kg	Fixed	0.5		0.5	
III	k_1	N/m	Fixed	33000		33000	0.2647
	k_2	N/m	Fixed	72100		72100	
	α	mm	Free	3	6	4.2	
	m_a	kg	Fixed	0.5		0.5	

Table 5.2: Optimization of 4 parameters

The main mass response for the best parameters is compared with LTVA , FTVA and WOTVA to understand how the optimization has impacted on widening of the frequency response at anti-resonance point. Here, Fixed Tuned Vibration absorber (FTVA) refers to locking of the auxiliary mass to main mass and WOTVA refers

to without any TVA. RMS values of displacement of main mass in all the above mentioned cases for optimized parameters are shown in Figure.5.7. It is observed that ATVA for optimum parameters shows a faltened main mass response in the operating frequency range of (40 - 47 Hz).

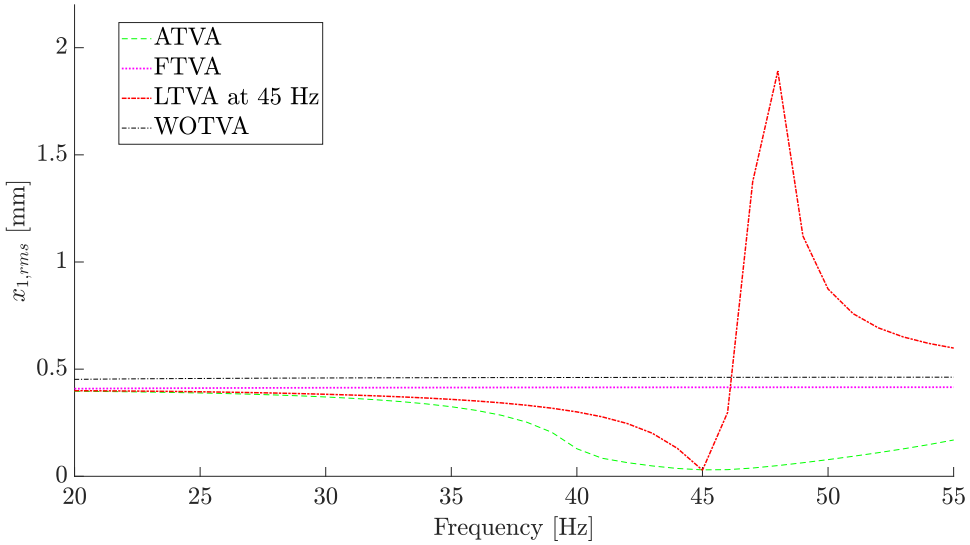

Figure 5.7: *Main mass response for optimized parameter set-* $k_1 = 33 \times 10^3\,\mathrm{N/m}, k_2 = 72.1 \times 10^3\,\mathrm{N/m}, \alpha = 4.2\,\mathrm{mm}, m_a = 0.5\,\mathrm{kg}$

5.2 ATVA - Activation

The idea of introducing a soft spring with stiffness k_1 was to ensure that the auxiliary mass starts moving as soon as the excitation begins. The optimized parameters has to be checked for activation. This was performed by simulating the response for a different start condition. The start condition here refers to how the excitation frequency and force is varied from rest position. Excitation force and frequency are varied according to Equation.5.9 and 5.10.

$$f = \begin{cases} f_{max} sin(\beta t), t \leq t_s \\ f_{max}, t > t_s \end{cases} \tag{5.9}$$

where $\beta = \dfrac{\pi}{2t_s}$, t_s is the time in which the maximum operating frequency is attained.

$$F_{e,RS} = \begin{cases} F_{e,ref} \left(\dfrac{f}{f_{ref}}\right)^2 sin(2\pi f t), t \leq t_s \\ F_{e,ref} \left(\dfrac{f_{max}}{f_{ref}}\right)^2 sin(2\pi f_{max} t), t > t_s \end{cases} \tag{5.10}$$

The response of ATVA is computed while the excitation begins from rest and reaches to a constant maximum. In Equation.5.9 it is assumed that excitation frequency

increases harmonically with time until it attains the maximum frequency. This assumption is close to reality because of the fact that the speed of moving blade in reciprocating saw (slider) increases harmonically. Further, it was assumed that the time taken to reach maximum excitation (t_s) as 1 s. Hence the excitation frequency is increased from 0 to maximum value of 47 Hz according to Equation.5.9 while the excitation force is computed according to Equation.5.10 wherein frequency term (f) is used from Equation.5.9. Note that the amplitude of excitation force at time greater than t_s becomes constant value. In Figure.5.8a and Figure.5.8b the frequency and excitation force for a simulation time of 2 s is shown.

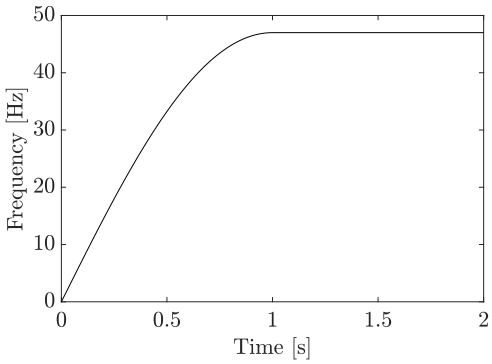

(a) *Excitation frequency*

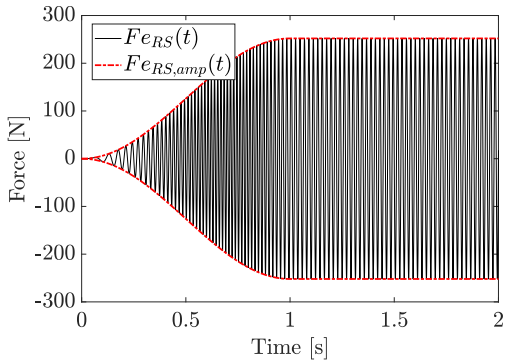

(b) *Excitation Force*

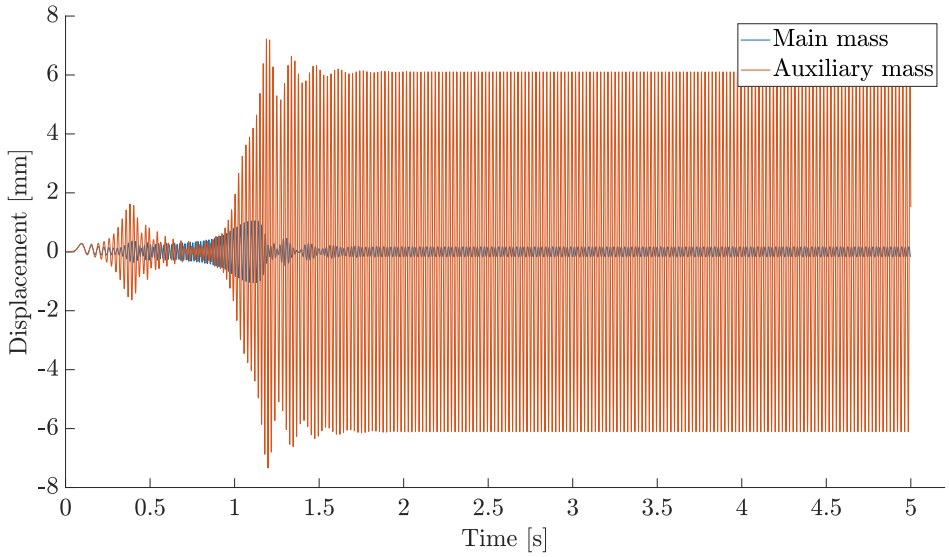

(c) *Model Response*

Figure 5.8: *Verification of ATVA activation*

The response of ATVA for above mentioned input force is shown in Figure.5.8c. It is observed that the auxiliary mass starts to move as soon as the excitation begins and the response of main mass is suppressed to a peak amplitude of 0.17 mm. This shows that ATVA can influence in suppressing the vibration of main mass.

5.3 Robustness

Actual input to the E-model always vary based on the usage of reciprocating saw and one has to understand how the ATVA behaviour varies for a change in the input force. Also, it is vital to check the ATVA behaviour when auxiliary damping is varied from the assumption made in optimization ($c_a = 1\,\mathrm{Ns/m}$). Basically, one can analyze the robustness of ATVA by looking into the objective function when the input force and auxiliary damping is varied. This helps to establish the limit on auxiliary damping which would still reduce vibration on main mass but not a optimum suppression. In reality, one has to measure the damping in ATVA to be sure of ATVA performance. Figure.5.9 shows the contour plot of objective function for different input force and auxiliary damping values.

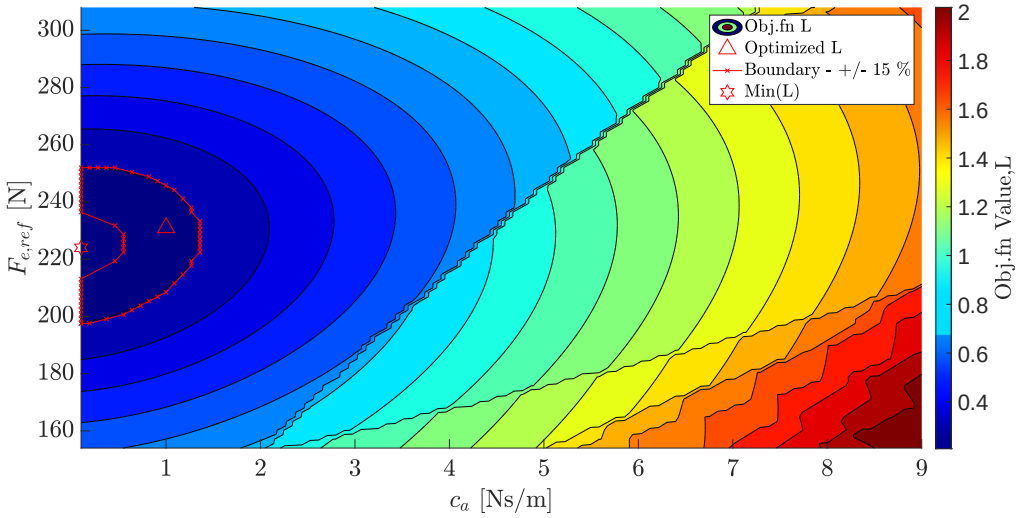

Figure 5.9: Contour Plot of Objective function for different input force and auxiliary damping

In Figure.5.9 auxiliary damping value is varied from 0.1 Ns/m to 9 Ns/m while the input force is varied from 154 N to 308 N. It is observed that the objective function attains the minimum value of 0.2081 when the auxiliary damping is set to 0.1 Ns/m (marked as $\star$). In reality it is very difficult to have such low damping. The red boundary in the contour plot shows a $\pm 15\%$ change in objective function form the optimized value (optimum objective function value is marked as $\triangle$). This boundary shows the acceptable ATVA operation. The boundary shown in the contour plot is acceptable because ATVA response inside this boundary is far better than a LTVA tuned at nominal frequency(45 Hz).

6
Conclusion

This chapter explains the results and describes how the vibration problem is solved in reciprocating saw with the aid of ATVA and also suggestions are made which can be used for further development.

The main objective of this project was to develop ATVA prototype for reciprocating saw (SR 30 A-36). First task was to identify the source of vibration in reciprocating saw. It was found that the reciprocating saw under consideration had a vibration reduction mechanism with an eccentric mass on the rotor of the saw. The eccentric mass created counteracting force to the cutting force and thus reducing vibrations to some extent. Unfortunately, the counter mass on the rotor could not be measured. On the other hand the added eccentric mass also created unwanted vibrations in a direction perpendicular to cutting. Hence, the plan to reduce overall vibrations was to eliminate the eccentric mass and add ATVA to the reciprocating saw.

A prototype of ATVA for a similar reciprocating saw was constructed in RISE with a non-linear stiffness. In the current existing prototype the non-linearity was created using single linear spring and gap. This prototype did not work due to the fact that the auxiliary mass was unable to move within the gap. Hence an additional spring was planned to introduce in ATVA prototype. For easy activation of ATVA, the additional spring should have relatively low stiffness and one has to investigate what stiffness value will be optimum for the range of excitation frequencies which the reciprocating saw will experience while cutting different materials. To be able to calculate the system parameters of ATVA, it is very crucial to identify what are the excitation forces and excitation frequencies. Hence a force measurement was made while running the reciprocating saw freely, cutting chipboard and cutting metal-pipe. The average from all the three measurements was used to arrive at a single force. The measured force was used as input to the engineering model and optimization of ATVA parameters such as soft spring(k_1), hard spring (k_2), auxiliary mass (m_a) and gap (α) was performed using the optimization algorithm developed in [7]. The optimized parameters were later used in developing the ATVA prototype. Minor changes were made in the old prototype to be able to fit in additional spring. Appendix.C shows the ATVA prototype construction and drawings.

The best part of ATVA is that it is capable to adjust to the excitation force. This was tested by varying the input force and auxiliary damping to see how the the objective function used for optimization varies. From the studies, it suggested that the ATVA with tuned parameters are robust with respect to the excitation force to

an extent of 10%. This means that for ±10% variation in the excitation force the performance of ATVA would change by 9%.

Finally, with the simulation results one can conclude that frequent problems related to vibrations in machine tool such as reciprocating saw can be addressed with ATVA. From the measurements it was found out that the reciprocating saw experiences a maximum peak to peak vibration amplitude of 1.2 mm. On implementing ATVA, simulations show that the vibration amplitude on the reciprocating saw can be lowered to a peak to peak amplitude of 0.34 mm.

ATVA was tested in free run condition to observe its capability in vibration attenuation. The test setup and the results are shown in Appendix.D. From test results, it was observed that the counter phase motion of auxiliary mass was predominant in Speed-1 when compared to Speed-2. This shows that at Speed-1, ATVA behaves in linear region and later at Speed-2 due to insufficient relative displacement, ATVA was not fully activated. This indicate that the auxiliary damping plays vital role in activating the ATVA. This was confirmed by comparing simulation result for increased auxiliary damping with test results. Auxiliary damping of 10 Ns/m gave results which was comparable with test result. Also, the discrepancies in the simulation and test results are due to the fact that the ATVA is rigidly fixed to main mass in simulation and it is not the case in reality. Damping in ATVA is mainly due to friction between moving auxiliary mass(m_a) & stationary housing. Secondly, the aerodynamic drag caused due to movement of auxiliary mass (m_a) inside confined housing also influences the auxiliary damping (see Appendix.C for ATVA construction). Further, to achieve fairly good vibration attenuation, friction between moving parts have to be substantially reduced.

6.1 Future Work

The next phase of the project work is to perform testing of the prototype in different situations and the simulation results have to be co-related. In this way one can improve the understanding of ATVA in reality. The most important part in the testing is to identify the influence of auxiliary damping in ATVA. Auxilliary damping has a great influence on performance of ATVA and was observed while performing prototype test. Also, one could do measurements on reciprocating saw when the eccentric mass on the rotor is removed to get more realistic input data. With new input data, the ATVA parameters have to be calculated and simulations of the same would give more hints on the maximum possible vibration suppression in reciprocating saw.

In this thesis work the optimization was performed for an input force which was computed by taking average of all three measurements(free run, chipboard cut and metal pipe cut). In future, the objective function used in the optimization routine could be changed a bit by giving some weights on the input force and thus making the parameters little more robust. The excitation force generated while cutting is assumed to be sinusoidal and in reality it should be more like a square wave. The

square wave nature of the excitation force is due to the fact that the blades are tilted with respect to slider axis and cut is produced while the blade retracts from work-piece. These updates on excitation force can be performed to obtain a new set of system parameters.

In future, the ATVA prototype manufacturing should take the surface finish into account. The inner surface of the ATVA cover and the outer surface of the auxiliary mass has to be really smooth. The surface finish greatly influence the friction between them and thereby auxiliary damping. Possible solution to achieve smooth surface is to perform grinding operation after machining of the surfaces.

Bibliography

[1] S.Hewitt, H.Mason. *A critical review of evidence related to hand-arm vibration syndrome and the extent of exposure to vibration*. Tech. rep. Health and Safety Executive, 2015.

[2] L. Aarhus, K. B. Veiersted, K.-C. Nordby, R. Bast-Pettersen. "Neurosensory component of hand–arm vibration syndrome: a 22-year follow-up study". In: *Occupational Medicine* (2019), 215–218.

[3] Mariantonieta Gutierrez Soto, Hojjat Adeli. "Tuned Mass Dampers". In: *Archives of Computational Methods in Engineering* (2013), 419–431.

[4] H. Frahm. *Device for damping vibrations of bodies. US989958*. 1911.

[5] H. Lindell. *Impact machine". WO2014095936A1*. 2014.

[6] H.Lindell, V.Berbyuk, M.Josefsson, S.L.Grétarsson. "Non-Linear Dynamic Absorber to reduce Vibration in hand held impact machines". In: *International Conference on Engineering Vibration* (2015), 1530–1539.

[7] M.Josefsson, S.L.Grétarsson. "Optimisation of a non-linear tuned vibration absorber in a hand-held impact machine". MA thesis. Department of Applied Mechanics: Chalmers Univeristy of technology 2015:19, 2015.

[8] A.Näkne. "Investigation of feasibility of Auto Tuning Vibration Absorber". MA thesis. Department of Applied Mechanics: Chalmers Univeristy of technology 2018:03, 2018.

[9] Alessandro Carrella. *Passive Vibration Isolators with High-Static-Low-Dynamic-Stiffness*. 2008.

[10] Stephen.P Loehnertz , Iris Vazquez. *Sawtooth Forces in Cutting Tropical Hardwood Native to South America*. 1998.

[11] E.Rodriguez, M.Paredes, M.Sartor. *Analtical Behavior Law for a Constant Pitch Conical Compression Spring*. 2006.

[12] *The Spring Catalogue-Lesjöfors*.

[13] J.P.Den Hartog. *Mechanical Vibrations*. 1956.

[14] Viktor Berbyuk. *Structural Dynamics Control*. Chalmers Univeristy of Technology, Göteborg, 2014.

[15] J. Ormondroyd, J.P.Den Hartog. *Theory of the dynamic vibration absorber*. 1928.

[16] J.E. Brock. *A Note on the Damped Vibration Absorber*. 1946.

[17] T. Asami,O. Nishihara. *Closed-Form Exact Solution to H Optimization of Dynamic Vibration Absorbers (Application to Different Transfer Functions and Damping Systems)*. 2003.

[18] J.B Hunt , J.C. Nissen. *The Broadband Dynamic Vibration Absorber*. 1982.

[19] Xingjian Jing, Zigiang Lang. *Frequecy Domain Analysis and Design of Non-Linear Systems based on Volterra Series Expansion*. 2014.

[20] *Understanding FFTs and Windowing*. https://download.ni.com/evaluation/pxi/Understanding%20FFTs%20and%20Windowing.pdf. [Online; accessed 15-March-2020].

[21] KERTÉSZ Milan, PALČÁK František. "The Role of the Stiffly Stable Integrators in Non-Linear Dynamic Simulations". In: *APLIMAT*. 2015.

[22] *Product Catalog-Hilti*. https://www.hilti.se/medias/sys_master/documents/h10/ha6/9477107580958/Operating-Instruction-SR-30-A36-01-Operating-Instruction-PUB-5391396-000.pdf. [Online; accessed 20-February-2020].

[23] *Tracker-Video Analysis and Modeling Tool*. https://physlets.org/tracker/. [Online; accessed 03-March-2020].

A

Kinematic Analysis of Slider Crank Mechanism

The reciprocating saw works on the principle of slider crank mechanism. The kinematic analysis of the mechanism is presented in this section. Figure A.1 shows the schematic arrangement of different links in the mechanism. The crank is drvien by an electric motor and is represented as OA. The connecting rod which connects the crank to slider is represented as AB. This mechanism has one degree of freedom which is the linear reciprocating motion of the slider. The generalized co-ordinate for analyzing the mechansim is θ.

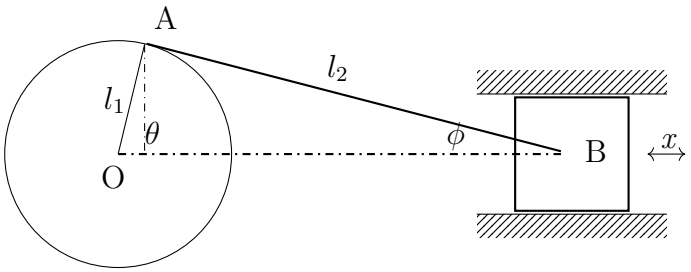

Figure A.1: *Schematic Representation of Slider Crank Mechanism in Reciprocating Saw*

The angle made by connecting rod AB with respect to line joining center of crank and slider OB is expressed as ϕ. This secondary angle ϕ can be expressed in terms of θ by applying *Sine rule* and is given as,

$$\frac{l_1}{sin(\phi)} = \frac{l_2}{sin(\theta)} \tag{A.1}$$

The displacement of the slider is written as a function of crank angle $\theta(t)$,

$$x(t) = l_1 cos(\theta(t)) + l_2 cos(\phi(t)) \tag{A.2}$$

On substituting Equation A.1 in Equation A.2 the displacement of the slider at any time instant is given as,

$$x(t) = l_1 cos(\theta(t)) + l_2 \sqrt{1 - \left(\frac{l_1 sin(\theta(t))}{l_2}\right)^2} \tag{A.3}$$

Differentiating Equation A.3 with respect to time gives the velocity of the slider $\dot{x}(t)$,

$$\dot{x}(t) = \frac{dx(t)}{dt} = \frac{dx}{d\theta}\frac{d\theta}{dt} = \omega\left[-l_1 sin(\theta(t)) - \frac{l_2\left(\frac{l_1}{l_2}\right)^2 sin(2\theta(t))}{2\sqrt{1-\left(\frac{l_1 sin(\theta(t))}{l_2}\right)^2}}\right] \tag{A.4}$$

Similarly, differentiating Equation A.4 gives acceleration of the slider $\ddot{x}(t)$ as a function of crank angle,

$$a = \omega^2\left[-l_1 cos(\theta(t)) - \left[\frac{l_1^2 cos(2\theta(t))}{l_2\left[\left(1-\left(\frac{l_1 sin(\theta(t))}{l_2}\right)^2\right)^{\frac{1}{2}}\right]} + \frac{l_1\left(\frac{l_1}{l_2}\right)^3[sin(2\theta(t))]^2}{4\left(1-\left(\frac{l_1 sin(\theta(t))}{l_2}\right)^2\right)^{\frac{3}{2}}}\right]\right] \tag{A.5}$$

B

Acceleration Measurements

The accelerations experienced by reciprocating saw while freely running, cutting chipboard, metal pipe was measured using two accelerometers. The accelerometer details and its sensitivity are given in the Table. B.1

Sensor		Model 3023A1, S/N 12545	Model 3023A1, S/N 12547
Sensitvity mV/g	X	10.48	10.68
	Y	10.68	10.09
	Z	10.42	10.91

Table B.1: *Sensitivity of Accelerometers*

The measurement setup is shown in the Figure. B.1. The accelerations are recorded in a computer using signal express software by National Instruments. The sensitivity of the accelerometers are entered in the software for processing the signal. Each accelerometer has 3 outputs and each output corresponds to direction in X,Y and Z axis or 1,2 and 3.

Figure B.1: *Measurement Setup with Accelerometers mounted on Reciprocating Saw*

Position of accelerometers are decided based on the flat surface available on the machine. The idea is to measure the accelerations as close as to cutting action and at the handle of the machine. The final selected place for mounting the accelerometers are shown in the Figure. B.2 and Figure. B.3

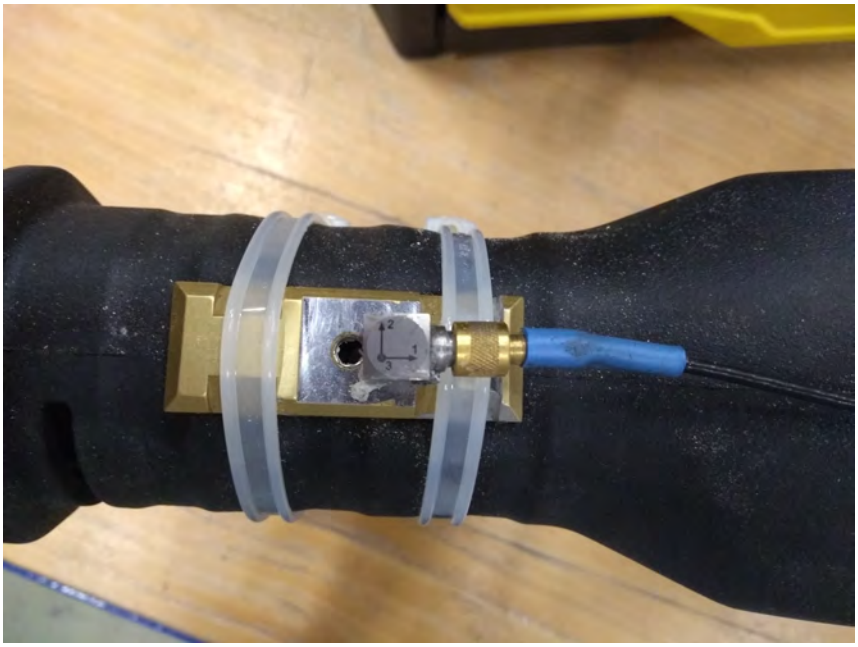

Figure B.2: *Accelerometer - 1 position on the reciprocating Saw*

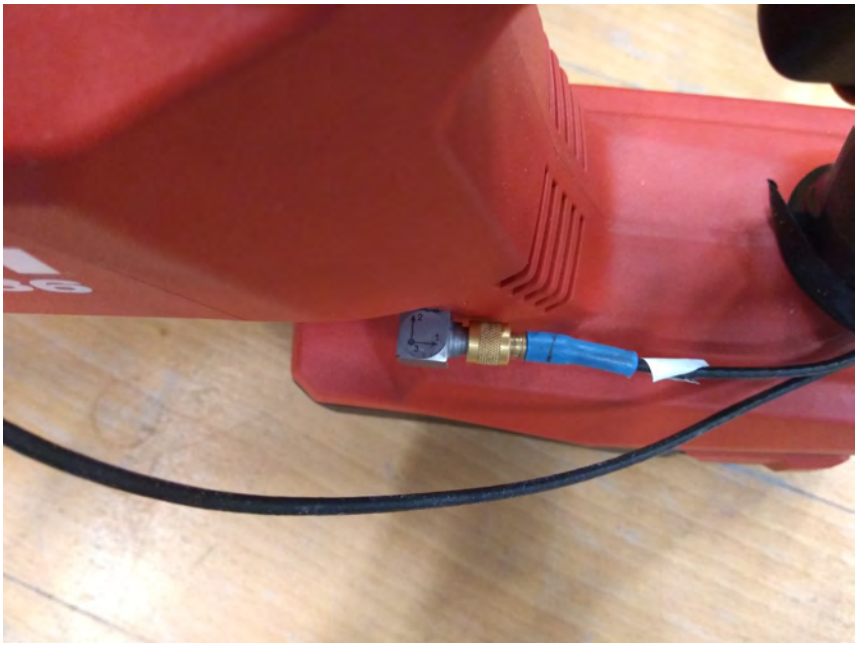

Figure B.3: *Accelerometer - 2 position on the reciprocating Saw*

Output from the sensors are connected to a data acquisition box. This is connected to a laptop and the data is accessed via Signal Express software. The trigger to

start the measurements were manually controlled in the software with the help of Snævar Leó Grétarsson.

To verify the measurements at free run, a slow motion video was made using high speed camera at ambient sunlight. The idea was to track a point on the surface of the reciprocating saw while operating at maximum speed,cf.Figure.B.4. The video was recorded for 2 seconds at 1000 frames per second. Later the camera data was analysed in a Tracker software [Video Analysis and Modelling Tool], Version 5.1.3. This Tracker software is an open source code and was downloaded from [23].To measure the amplitude of vibration, the input to the tracker software was given as pixel points on the yellow coloured tape.

Figure B.4: *Tracking a point on Reciprocating Saw using High speed camera*

Figure B.5: *Chipboard used for cutting (*38 mm *thick)*

Figure B.6: *Metal Pipe used for cutting-*2 mm *thick*

C

ATVA Prototype

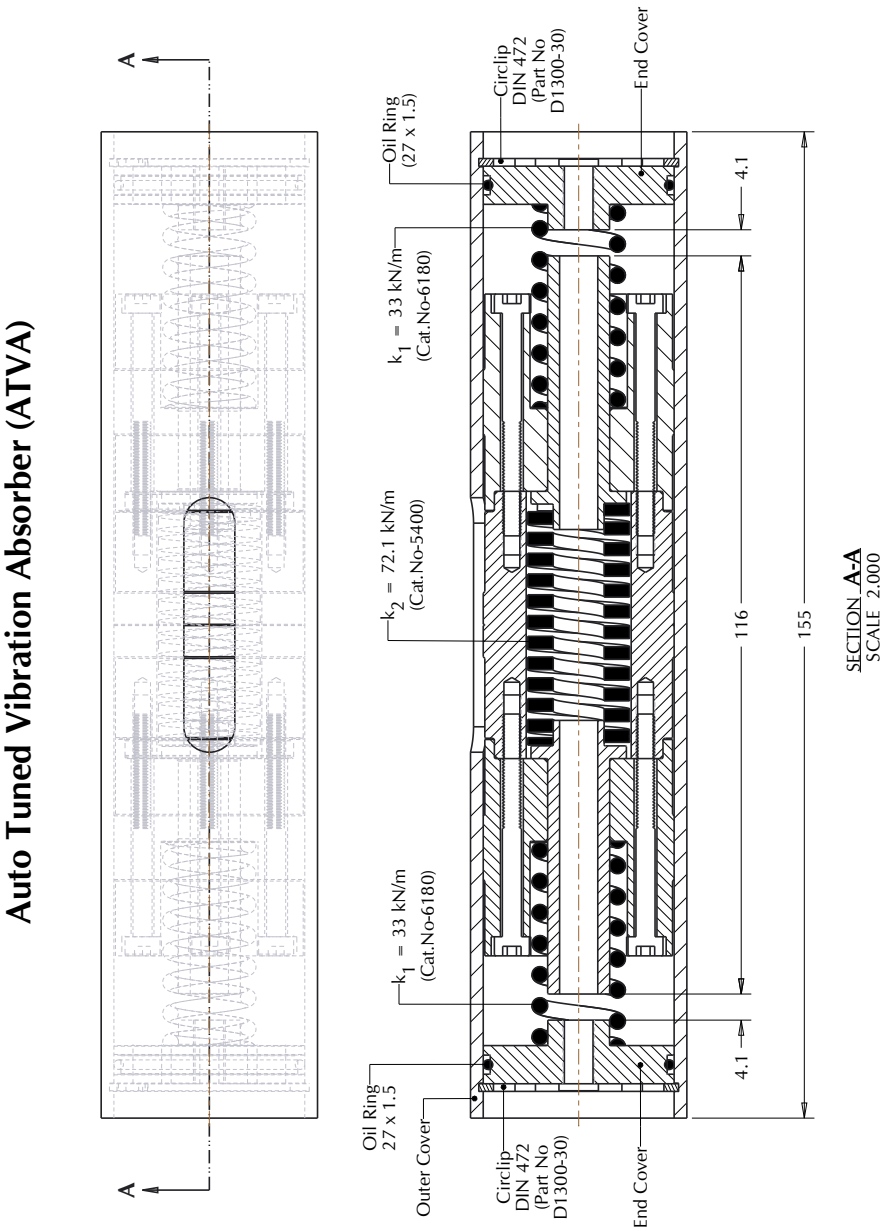

Figure C.1: *ATVA Prototype Assembly drawing*

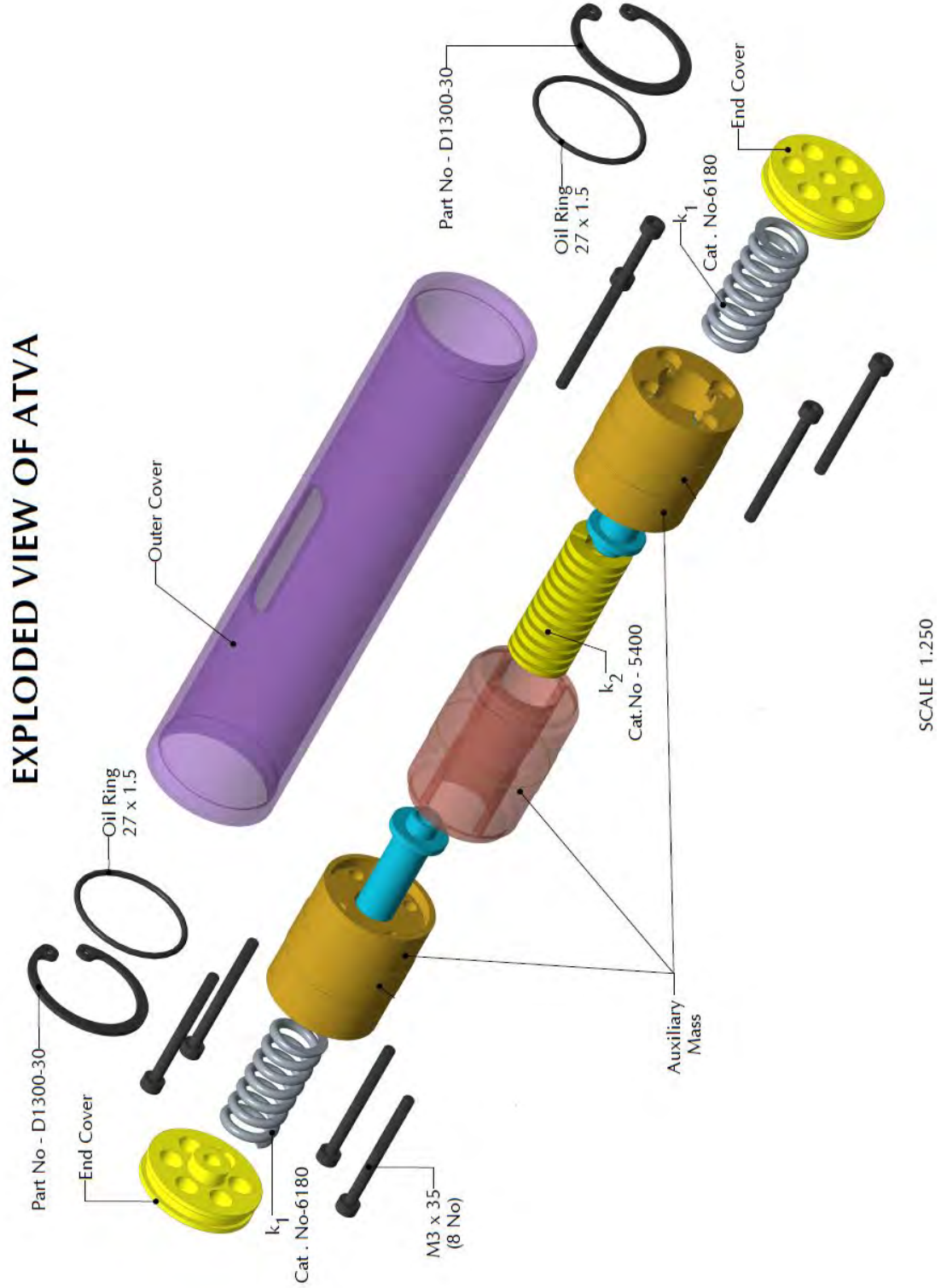

Figure C.2: *ATVA Prototype - Exploded View*

D

ATVA Prototype Test

ATVA is mounted on the reciprocating saw using a 'L' shaped bracket. The bracket is held rigidly to the reciprocating saw using metal hose clip. Hot glue is used on the other end of ATVA to hold it securely. Figure.D.1 shows ATVA mounted on the reciprocating saw.

Figure D.1: *ATVA Test Setup*

ATVA was tested at two speed levels while running at maximum capacity. The movement of reciprocating saw and auxiliary mass was captured using a camera to analyze the effect of ATVA on reciprocating saw using tracker software.

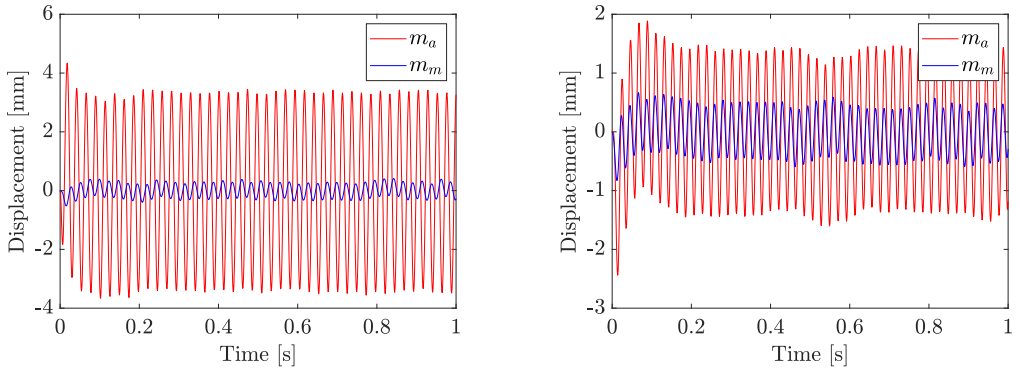

(a) *Speed -1* **(b)** *Speed -2*

Figure D.2: *ATVA Prototype Test results for free run*

The testing revealed that the ATVA is not fully activated at Speed-1 and Speed-2. In Speed level 1 the counter phase motion of auxillary mass with respect to main mass can be observed. In speed level-2 the auxillary mass is not in counter phase motion. This can be explained by the auxillary damping in comparision to simulation and actual test. In reality, the friction between the auxillary mass and the outer tube is significant and hinders the activation of ATVA.